

The helium atom in a strong magnetic field

W.Becken, P.Schmelcher and F.K. Diakonos*

Theoretische Chemie
Physikalisch-Chemisches Institut
Im Neuenheimer Feld 253
69120 Heidelberg
Federal Republic of Germany

Abstract

We investigate the electronic structure of the helium atom in a magnetic field between $B = 0$ and $B = 100a.u.$. The atom is treated as a nonrelativistic system with two interacting electrons and a fixed nucleus. Scaling laws are provided connecting the fixed-nucleus Hamiltonian to the one for the case of finite nuclear mass. Respecting the symmetries of the electronic Hamiltonian in the presence of a magnetic field, we represent this Hamiltonian as a matrix with respect to a two-particle basis composed of one-particle states of a Gaussian basis set. The corresponding generalized eigenvalue problem is solved numerically, providing in the present paper results for vanishing magnetic quantum number $M = 0$ and even or odd z -parity, each for both singlet and triplet spin symmetry. Total electronic energies of the ground state and the first few excitations in each subspace as well as their one-electron ionization energies are presented as a function of the magnetic field, and their behaviour is discussed. Energy values for electromagnetic transitions within the $M = 0$ subspace are shown, and a complete table of wavelengths at all the detected stationary points with respect to their field dependence is given, thereby providing a basis for a comparison with observed absorption spectra of magnetic white dwarfs.

1 Introduction

Since the astrophysical discovery of strong magnetic fields on the surfaces of white dwarfs ($\leq 10^5$ Tesla) and neutron stars ($\approx 10^8$ Tesla) the interest in the behaviour and the properties of matter in strong magnetic fields has increased enormously. In the case of atoms in strong magnetic fields most of the literature is concerned with the hydrogen atom. The eigenvalues and the eigenfunctions of the hydrogen atom are, therefore, known very precisely and for many excited states [1–7]. For the hydrogen atom in a strong magnetic field it was possible to perform a comparison of the theoretical predictions resulting from *ab initio* computations with the data obtained from astronomical observation. The results provided an overwhelming evidence for the existence of hydrogen in the atmosphere of the corresponding astrophysical objects [6]. However, there are several spectral features and structures which can not be explained by hydrogenic spectra like for example in the spectrum of the magnetic white dwarf GD229 [8–10], which leads to the conjecture that there are further components in the atmospheres, i.e. atoms with more than one electron.

*Permanent address: Department of Physics, Univ. of Athens, GR-15771 Athens, Greece

So far our knowledge about atoms with more than one electron in strong magnetic fields is very sparse. Most of the *ab initio* computations on more electron systems deal with two-electron systems, i.e. the helium atom, the hydrogen anion and the helium-like kations [6, 11–14]. For two-electron atoms the investigations cover much smaller parts of the spectrum than it is the case for the hydrogen atom, and their accuracy is considerably poorer. To perform a comparison with astrophysical observation, however, accurate transition energies for a large set of field strengths have to be available which requires even more accurate data for the total energies. In particular in the relevant regime of intermediate field strengths, for which the diamagnetic energies and the Coulomb energies are of the same order of magnitude, there does not exist sufficiently accurate data for a large number of excited states which would allow this comparison. The reason is that for example the numerical basis set methods established so far have their starting point either in the low-field regime or in the high-field regime and are, therefore, especially adapted to their corresponding regimes but fail to be effective in the opposite regime, thereby leaving a gap in a certain regime where none of them provides a good convergence.

The scope of the present paper is to introduce one uniform basis set method which is capable of accurately describing two electron systems for arbitrary field strengths. We present numerical results for the energy levels of the ground state and a considerable number of excited states of the helium atom in a magnetic field ranging from $B = 0$ a.u. to $B = 100$ a.u. ($B = 1$ a.u. corresponds to $2.35 \cdot 10^5$ Tesla).

In order to perform a detailed comparison of our numerical data with already existing ones, let us first provide an overview of the results present in the literature so far. Almost all of the results we mention here are variational, i.e. they provide upper bounds for the exact energy values. However, we have to distinguish between Hartree-Fock calculations and calculations which take into account the electronic correlation.

The first Hartree-Fock calculations on helium in a strong magnetic field have been performed in 1976 by Virtamo [15]. Virtamo has provided the global ground-state energies of helium in very strong fields ($B = 80$ a.u. up to $B = 8 \times 10^4$ a.u.). In this regime the lowest energy is achieved by aligning both spins antiparallel to the magnetic field which means that the global ground state in question is a spin triplet state. The same state is also investigated in the work of Pröschel et al. [12]. They use a Slater-determinantal approach starting from Landau-levels in order to cover a slightly broader regime of field strengths as Virtamo ($B \sim 2.1$ a.u. to $B \sim 2.1 \times 10^4$ a.u.). Hartree-Fock results for several other states besides the ground state of helium in the high-field regime are provided in the works of Ivanov [14, 16] where the singlet and triplet states are considered for positive total z -parity and magnetic quantum numbers $m = 0, -1$ as well as for negative z -parity and $m = 0$. Here the magnetic field ranges from $B = 0$ a.u. to $B = 100$ a.u. occupying 11 field strengths and thus includes both the low-field and high-field regime as well as the intermediate regime. On an even finer grid of field strengths (34 values between $B = 8 \times 10^{-4}$ a.u. and $B = 8 \times 10^3$ a.u.) the energies of the triplet ground state and several triplet excited states but no singlet states are given in the work of Thurner et al. [13]. In the latter work there exists a gap in the list of eigenenergies for several states in the vicinity of $B \sim 1$ a.u. because the ansatz of the applied approach changes in the intermediate regime from a spherical to a cylindrical symmetry and thus fails to provide accurate results in the intermediate regime. An important work is also the Hartree-Fock study of Jones, Ortiz and Ceperley [17]. They present the HF-energies for the global low-field ground state for various field strengths between $B = 8 \times 10^{-4}$ a.u. and $B = 8$ a.u. and thus also address the intermediate regime. They additionally provide energies for several excited states (but those results are crude approximations providing no upper bounds).

In comparison to the considerable number of Hartree-Fock investigations there are much less data available on fully correlated calculations of helium so far. Mueller, Rau and Spruch [18] obtain variational upper-bound estimates of the binding energies of the triplet states with negative z -parity and the magnetic quantum numbers $m = 0$ and $m = -1$ and of the singlet ground state which has positive z -parity and $m = 0$. Their field strengths range from $B \sim 4.2$ a.u. to $B \sim 2.1 \times 10^4$ a.u.. A similar high-field regime

($B = 4.2\text{a.u.}, 42\text{a.u.}, 420\text{a.u.}$) is addressed by the work of Vincke and Baye [19] which also presents variational estimates for binding energies. They consider the singlet and triplet states for positive z -parity and $m = 0, -1, -2$. The first correlated calculations in the intermediate regime have been provided by Larsen [20] who has given the energies of the singlet states with positive z -parity and $m = 0, -1$ or with negative z -parity and $m = 0$ as well as the triplet ground state for the four field strengths $B = 0.2, 0.5, 1.0, 2.0\text{a.u.}$. Park and Starace [21] have computed upper and lower bounds for the singlet ground state in the low-field regime between $B = 0\text{a.u.}$ and $B = 0.15\text{a.u.}$. Recently, Jones, Ortiz and Ceperley [22] have applied a released-phase quantum Monte Carlo method to the helium atom. Energies for spin triplet states with both positive and negative z -parity and $m = 0, -1$ are given for field strengths from $B = 0\text{a.u.}$ up to $B = 8.0\text{a.u.}$. Though in principle the results of those investigations are variational their numerical values must be handled with care when using them as upper bounds for the helium energies. The reason is that due to the statistical character of their method the results possess error bars which might trespass the exact values of the helium energies. Very recently the finite-element technique has as well been used to calculate energies for several singlet and triplet states of helium in a magnetic field[23]. Also this approach does not provide a significant improvement.

In the present work we use a Gaussian basis set method which permits to perform *fully correlated* calculations on singlet and triplet states of helium with arbitrary spatial symmetry. This basis set method has been developed by Schmelcher and Cederbaum [24] for molecules and has already successfully been applied to the hydrogen molecule ion [25] and to the neutral hydrogen molecule [26, 27] in strong magnetic fields. We translate this basis set in order to be applicable to ab initio calculations of atoms in strong magnetic fields. We remark that using for example a Hylleraas basis set yields more accurate results in the field-free or weak-field case due to explicitly correlated orbitals. However, it is not efficient and accurate in the presence of a strong magnetic field due to the spherical symmetry of the exponentials [28]. In contrast to this our basis set described in detail in sec. III below can be adapted to any field strength.

All the helium states considered are classified according to a maximal set of conserved quantities, which we choose to be the total spin S^2 , the z -component S_z of the total spin, the total spatial magnetic quantum number M and the total spatial z -parity Π_z . For twenty field strengths from $B = 0\text{a.u.}$ up to $B = 100\text{a.u.}$ numerical helium energies for singlet and triplet states are given for $M = 0$ and for $\Pi_z = 0, 1$. In each of these two subspaces we present the energies of the ground state and the first five excited states for singlet and four excited states for triplet spin symmetry. The accuracy of our method in the field-free case can be determined by comparison of our results with the very precise field-free values calculated by Braun et al.[29], Accad et al.[30] or by Drake et al.[31], and our relative deviation ranges from 10^{-6} to 10^{-4} . We do not observe this accuracy to drop considerably with increasing magnetic field, which means that our basis set method produces accurate results in particular in the intermediate regime. Both with respect to the achieved relative accuracy as well as with respect to the number of excited states our investigation provides therefore valuable results. Data for $M \neq 0$ will be presented in a future work. The stationary components of the transitions obtained in the present investigation provide an important part of the data which have very recently been used to show the presence of helium in the atmosphere of the magnetic white dwarf GD229[10].

In detail we proceed as follows. In section II we discuss the influence of the finite nuclear mass, i.e. the scaling relations which connect the Hamiltonian for a finite nuclear mass to a Hamiltonian with infinite nuclear mass. In all of the remaining sections, we consider the nonrelativistic case with infinite nuclear mass and an electron spin g -factor equal 2. Section III starts with the nonrelativistic Hamiltonian of a helium atom with infinite nuclear mass in a magnetic field. The corresponding symmetries of this Hamiltonian are discussed and serve for constructing a suitable basis set. The matrix representation of the Hamiltonian with respect to this basis gives rise to an eigenvalue problem. The results of its diagonalization are discussed

in section IV where we present total energies, ionization energies and transition energies as well as the wavelengths of their stationary components, all of them given under the assumption of infinite nuclear mass.

2 Finite nuclear mass scaling relations and further corrections

We use a nonrelativistic approach to the helium atom. This is justified because the relative changes in the helium energies due to relativistic effects are smaller than the relative accuracy of our nonrelativistic energies [32]. Additionally for simplicity we use an electron spin g -factor equal 2 throughout the paper. The following scaling laws as well as all of our numerical results can trivially be adapted to a g -factor of any desired accuracy by multiplying every occurring spin operator or eigenvalue with $\frac{g}{2}$.

Though our electronic structure calculations will be carried out with the assumption of an infinite nuclear mass, they can, by means of a scaling law, be translated into results with a finite nuclear mass. The latter are necessary in order to achieve the accuracy for a detailed comparison with astrophysical data. The idea to introduce such a scaling relation is not new but has already been applied to one-electron systems earlier [33]. In order to demonstrate how this idea is applied on the helium atom, we will start with the full Hamiltonian describing a neutral system with two interacting electrons with masses 1 and charge -1 in the Coulomb field of a nucleus with charge two and *finite* mass M_0 in a magnetic field \mathbf{B} . Assuming a vanishing pseudomomentum of the center of mass (see refs. [34–36] for a pseudoseparation of the center of mass motion for neutral systems in a magnetic field) one obtains the following exact pseudoseparated Hamiltonian (which is established in the symmetric gauge $\mathbf{A}(\mathbf{r}) = \frac{1}{2}\mathbf{B} \times \mathbf{r}$)

$$H_e = \sum_i^2 \left(\frac{1}{2\mu} \mathbf{p}_i^2 + \frac{1}{2\mu'} \mathbf{B} \cdot \mathbf{l}_i + \frac{1}{8\mu} (\mathbf{B} \times \mathbf{r}_i)^2 - \frac{2}{|\mathbf{r}_i|} + \mathbf{B} \cdot \mathbf{s}_i \right) + \frac{1}{|\mathbf{r}_2 - \mathbf{r}_1|} + \frac{1}{2M_0} \sum_{i \neq j} \left(\mathbf{p}_i \mathbf{p}_j - \mathbf{p}_i (\mathbf{B} \times \mathbf{r}_j) + \frac{1}{4} (\mathbf{B} \times \mathbf{r}_i) (\mathbf{B} \times \mathbf{r}_j) \right), \quad (1)$$

where $\mu = \frac{M_0}{M_0+1}$ is the reduced mass and $\mu' = \frac{M_0}{M_0-1}$ (we use atomic units throughout the paper). We take into account the dominant part of the finite mass corrections by introducing these quantities μ, μ' and neglect the mass polarization terms represented by the sum over $(i \neq j)$. Our basic idea is now find a scaling law joining the spectrum of the remaining part $H(M_0, B)$ in the first line of the Hamiltonian H_e with the spectrum of the infinite-mass Hamiltonian $H(\infty, \bar{B})$ at a suitable different field strength \bar{B} . The neglect of the mass polarization terms of the sum over $(i \neq j)$ in eq.(1) is justified by the fact that they are expected to provide a smaller correction to the total energy than the corresponding diagonal mass corrections, i.e. the replacement of the masses by reduced ones.

We will show how it is possible to establish a relation between the operators $H(M_0, B)$ and $H(\infty, \bar{B})$ themselves which is even more fundamental than only a relation between the corresponding spectra. The relation in question cannot be a simple Unitarian because such a transformation would leave the spectrum invariant. Instead, we will show that there is a unique way how to represent $H(M_0, B)$ in the form $UH(M_0, B)U^{-1} = \alpha H(\infty, \bar{B}) + \beta$, where α is a number and β is a suitable operator commuting with the Hamiltonian.

Before factoring out a suitable prefactor α the terms of $H(M_0, B)$ must be transformed in such a way that their mutual ratios possess the correct infinite-mass values, i.e. all ratios must neither contain μ nor μ' . The misproportion between the kinetic energy and the Coulomb energy terms is the only one which cannot be absorbed in the parameter B or be removed by separating a suitable additive operator β commuting with the Hamiltonian. Thus we are obliged to introduce the canonical scale transformation $\mathbf{r} \rightarrow \frac{1}{\mu} \mathbf{r}$, $\mathbf{p} \rightarrow \mu \mathbf{p}$ of

the coordinates themselves. We realize this transformation by the Unitarian $U = e^{-i\frac{\ln\mu}{2}(\mathbf{x}\mathbf{p}+\mathbf{p}\mathbf{x})}$, yielding

$$UH(M_0, B)U^{-1} = \mu \left[\sum_i^2 \left(\frac{1}{2}\mathbf{p}_i^2 + \frac{1}{8}(\frac{1}{\mu^2}\mathbf{B} \times \mathbf{r}_i)^2 - \frac{2}{|\mathbf{r}_i|} \right) + \frac{1}{|\mathbf{r}_2 - \mathbf{r}_1|} \right] + \sum_i^2 \left(\frac{1}{2\mu'}\mathbf{B} \cdot \mathbf{l}_i + \mathbf{B} \cdot \mathbf{s}_i \right) \quad (2)$$

The operator \mathbf{s}_i of the spin degree of freedom is not affected by the above transformation, and $\mathbf{l}_i = \mathbf{r}_i \times \mathbf{p}_i$ is also unchanged because the scaling factors of \mathbf{r}_i and \mathbf{p}_i cancel each other. The expression in square brackets is already an essential part of the desired infinite-mass Hamiltonian at the adjusted field strength $\bar{B} = \frac{1}{\mu^2}B$: only the Zeeman orbital and spin term at the field strength \bar{B} are missing. These operators can be provided by hand, which must be repaired by subtracting the same operators at the end where they almost cancel exactly the original Zeeman and spin terms leaving only a contribution of order $\frac{B}{M_0}$:

$$\begin{aligned} UH(M_0, B)U^{-1} = & \mu \left[\sum_i^2 \left(\frac{1}{2}\mathbf{p}_i^2 + \frac{1}{2}\bar{\mathbf{B}} \cdot \mathbf{l}_i + \frac{1}{8}(\bar{\mathbf{B}} \times \mathbf{r}_i)^2 - \frac{2}{|\mathbf{r}_i|} + \bar{\mathbf{B}} \cdot \mathbf{s}_i \right) + \frac{1}{|\mathbf{r}_2 - \mathbf{r}_1|} \right] \\ & + \sum_i^2 \left(-\mu\frac{1}{2}\bar{\mathbf{B}} \cdot \mathbf{l}_i - \mu\bar{\mathbf{B}} \cdot \mathbf{s}_i + \frac{1}{2\mu'}\mathbf{B} \cdot \mathbf{l}_i + \mathbf{B} \cdot \mathbf{s}_i \right) \end{aligned} \quad (3)$$

Therefore we obtain

$$UH(M_0, B)U^{-1} = \mu \cdot H(\infty, B/\mu^2) - \frac{1}{M_0}\mathbf{B} \cdot \sum_i(\mathbf{l}_i + \mathbf{s}_i) \quad (4)$$

In particular, the spectrum of $H(M_0, B)$ is identical with the spectrum of the unitarily equivalent operator represented by the right side of (4). The latter spectrum can be simply connected to the spectrum of $H(\infty, B/\mu^2)$ itself because the operators $\sum_i \mathbf{B} \cdot \mathbf{l}_i$ and $\sum_i \mathbf{B} \cdot \mathbf{s}_i$ commute with the Hamiltonian: we will use in the following section an angular momentum and spin basis, in the case of which the additional operator $-\frac{1}{M_0}\mathbf{B} \cdot \sum_i(\mathbf{l}_i + \mathbf{s}_i)$ gives rise to a trivial energy shift of order $\frac{B}{M_0}$.

3 Symmetries, Hamiltonian and Basis sets

3.1 Symmetries and Hamiltonian

In the following we assume the magnetic field to point in the $+z$ -direction. Then the Hamiltonian $H(\infty, B)$ for infinite nuclear mass at given field strength B (in the following we will omit the argument ' ∞ ') reads

$$H = \sum_{i=1}^2 \left(\frac{1}{2}\mathbf{p}_i^2 + \frac{1}{2}Bl_{zi} + \frac{B^2}{8}(x_i^2 + y_i^2) - \frac{2}{|\mathbf{r}_i|} + Bs_{zi} \right) + \frac{1}{|\mathbf{r}_2 - \mathbf{r}_1|} \quad (5)$$

The sum contains the one-particle operators, i.e. the Coulomb potential energies $-\frac{2}{|\mathbf{r}_i|}$ of the electrons in the field of the nucleus as well as their kinetic energies, already splitted into the part $\frac{1}{2}\mathbf{p}_i^2$, the Zeeman term $\frac{1}{2}Bl_{zi}$ and the diamagnetic term $\frac{B^2}{8}(x_i^2 + y_i^2)$, and their spin energies Bs_{zi} . The two-particle operator $\frac{1}{|\mathbf{r}_2 - \mathbf{r}_1|}$ represents the electron-electron repulsion energy.

There exist four independent commuting conserved quantities: the total spin \mathbf{S}^2 , the z -component S_z of the total spin, the z -component L_z of the total angular momentum and the total spatial z -parity Π_z . In the following calculations we consider separately each subspace of a specified symmetry, i.e. with given eigenvalues of \mathbf{S}^2 , S_z , L_z and Π_z .

3.2 The underlying one-particle basis set

The key ingredient of our basis set method is the Gaussian one-particle basis set which is our starting point for the construction of spatial two-particle states. According to the azimuthal symmetry with respect to the magnetic field axis, cylindrical coordinates are suitable for representing the one-particle basis functions

$$\Phi_i(\rho, \varphi, z) = \rho^{n_{\rho i}} z^{n_{z i}} e^{-\alpha_i \rho^2 - \beta_i z^2} e^{im_i \varphi} \quad i = 1, \dots, n, \quad (6)$$

where α_i and β_i are positive nonlinear variational parameters and the exponents $n_{\rho i}$ and $n_{z i}$ obey the following restrictions:

$$n_{\rho i} = |m_i| + 2k_i; \quad k_i = 0, 1, 2, \dots \text{ with } m_i = \dots - 2, -1, 0, 1, 2, \dots \quad (7)$$

$$n_{z i} = \pi_{z i} + 2l_i; \quad l_i = 0, 1, 2, \dots \text{ with } \pi_{z i} = 0, 1 \quad (8)$$

The basis function Φ_i is an eigenfunction of the z -component of the angular momentum with eigenvalue m_i and an eigenfunction of the z -parity with eigenvalue $(-1)^{\pi_{z i}}$. The Gaussian-like expression $\rho^{|m_i|} e^{-\alpha_i \rho^2}$ is identical with the ρ -dependence of the lowest Landau-state in the field B if we choose α_i to be $\frac{B}{4}$ and thus represents an adjustment to the existence of the magnetic field (see e.g. eq. (8) in [36]). The monomials ρ^{2k_i} and $z^{n_{z i}}$ are suitable for describing excitations. The flexibility of our basis set which permits us to choose suitably the values of the nonlinear parameters α_i and β_i is one of its major advantages: For low field strengths an isotropic choice $\alpha_i = \beta_i$ will be reasonable where the α_i, β_i cover a regime which allows the Φ_i to optimally approximate Slater-type orbitals. At high field strengths, however, where the magnetic field destroys the spherical symmetry of the problem, an isotropic basis set method would be inefficient. Here we choose the distribution of the α_i to be peaked around $\frac{B}{4}$ whereas the β_i are well-tempered in a large regime.

The best choice of the α_i and β_i has been computed by the requirement to solve optimally the one-particle problem of the H -atom or the He^+ -ion in a magnetic field of given strength B . To achieve this, we applied the following optimization procedure. For any given one-particle subspace (m, π_z) which will be involved in the later on two-particle configurations we have chosen a suitable number, typically 20, of functions of the type (6) with the same one-particle quantum numbers ($m_i = m, \pi_{z i} = \pi_z$) but different starting values α_i and β_i . With respect to this basis we built up the overlap matrix and the matrix of the one-particle Hamiltonian, representing a generalized eigenvalue problem for the one-particle energies. Now, we determined systematically the values of the α_i and β_i which minimized the energy eigenvalues of the one-particle ground state or a desired excited state. Our tool was a repeated reconstruction and diagonalization of the matrices directed by the pattern-search-method applied in the $\{\alpha_i, \beta_i\}$ space. We remark that due to the large number of parameters it is very time consuming to find the best selection of parameters $\{k_i, l_i\}$. Additionally the starting values for the nonlinear parameters α_i and β_i have to be chosen carefully in order to find a "good" minimum close to the global one on the complicated hypersurface.

3.3 The two-particle basis set

Our basic idea for solving the time-independent Schrödinger equation for the Hamiltonian (5) is to construct a basis set of suitable two-particle states $|q\rangle$ each of which is itself an eigenstate of the conserved quantities with eigenvalues M, Π_z, S, S_z , respectively. With respect to this not necessarily orthonormal basis we construct a matrix representation H_{pq} of the Hamiltonian and define an overlap matrix S_{pq} by

$$H_{pq} := \langle p | H | q \rangle \quad (9)$$

$$S_{pq} := \langle p | q \rangle \quad (10)$$

where the states $|p\rangle, |q\rangle$ lie in the *same* subspace of given eigenvalues of M, Π_z, S, S_z . By construction, the matrix $\underline{\underline{H}}$ is hermitian and the matrix $\underline{\underline{S}}$ is hermitian and positive definite. Additionally to these general properties, in the special case of the basis sets we use, all the matrix elements turn out to be real. By solving the finite-dimensional generalized real-symmetric eigenvalue problem

$$(\underline{\underline{H}} - E\underline{\underline{S}}) \cdot \underline{c} = 0 \quad (11)$$

we obtain eigenvectors \underline{c} whose corresponding eigenvalues E are strict upper bounds to the exact eigenvalues of the Hamiltonian (5) within the given subspace.

We choose our two-particle basis functions to be direct products of a pure spatial part $|\psi_q\rangle$ with a pure spin part $|\chi_q\rangle$:

$$|q\rangle = |\psi_q\rangle \otimes |\chi_q\rangle \quad (12)$$

The spin part is assumed to be one of the usual orthonormal singlet or triplet spin eigenstates. This means that the overlap matrix is nontrivial purely due the spatial part,

$$S_{pq} = \langle \psi_p | \psi_q \rangle, \quad (13)$$

and each matrix element of the Hamiltonian decomposes in a spatial and a spin contribution:

$$H_{pq} = \langle \psi_p | H_{spat} | \psi_q \rangle + S_{pq} \langle \chi_p | H_{spin} | \chi_q \rangle \quad (14)$$

The spin contribution $\langle \chi_p | H_{spin} | \chi_q \rangle$ is trivial and equals $+B \cdot S_z$, according to (5), and therefore it vanishes for singlet states or is either $-B, 0$ or $+B$ for triplet states. Due to its prefactor S_{pq} it can simply be absorbed as a shift in the energy eigenvalue E in eq.(11). Since a spin singlet state is antisymmetric and a triplet state is symmetric with respect to particle exchange, the spatial part associated to a spin singlet state must be symmetric whereas the spatial part associated to a spin triplet state must be antisymmetric.

In contrast to the spin part the spatial part is by no means trivial and it is an art to find a suitable finite-dimensional basis set for accurately approximating the Hilbert space of bound states of H_{spat} . This is the reason why we spent so much effort on providing a powerful one-particle basis set (see sec. 3.2). It serves now as a good starting point to compose the desired two-particle states. We choose a two-particle basis state to be

$$|\psi_q\rangle := b_i^\dagger b_j^\dagger |0\rangle \quad i = 1, \dots, n, \quad j = i, \dots, n, \quad (15)$$

where b_i^\dagger is a creation operator of the i -th one-particle basis state $|i\rangle = b_i^\dagger |0\rangle$ whose position representation is given by (6). This means that we will treat the helium atom by a **full Configuration Interaction (full CI)** approach within the one-particle basis set of states $|i\rangle$. Depending on whether the spin part $|\chi_q\rangle$ is a singlet or triplet state, the operators b_i^\dagger must be bosonic or fermionic, respectively.

Now, in order to establish a basis set of two-particle states spanning the subspace with the given pure values of the total magnetic quantum number M and the total z -parity Π_z , we must select all the combinations i, j with

$$m_i + m_j = M \quad (16)$$

$$\text{mod}(\pi_{zi} + \pi_{zj}, 2) = \Pi_z, \quad (17)$$

yielding a dimension N of the constructed two-particle basis set which is in general smaller than $\frac{n(n+1)}{2}$. We remark that for triplet spin symmetry those states in (15) with $i = j$ fail to exist which means that the dimension N for triplet subspaces is in general smaller than for singlet subspaces.

3.4 Matrix elements

In order to calculate the matrix elements of the Hamiltonian (5), we must rewrite its spatial part in second quantization, $\hat{H}_{spat} = \hat{H}_I + \hat{H}_{II}$, where \hat{H}_I and \hat{H}_{II} denote the second-quantized counterparts of the familiar one- and two-particle operators whose position representations read

$$H_I(\mathbf{p}, \mathbf{r}) = \frac{1}{2}\mathbf{p}^2 + \frac{1}{2}\mathbf{B} \cdot \mathbf{l} + \frac{1}{8}(x^2 + y^2) - \frac{2}{|\mathbf{r}|} \quad (18)$$

$$H_{II}(\mathbf{r}_1, \mathbf{r}_2) = \frac{1}{|\mathbf{r}_2 - \mathbf{r}_1|} \quad (19)$$

The next step now is to calculate the spatial matrix elements according to (14). With $|\psi_q\rangle := b_i^\dagger b_j^\dagger |0\rangle$ and $|\psi_p\rangle := b_k^\dagger b_l^\dagger |0\rangle$ a straightforward calculation leads to

$$\langle \psi_p | \psi_q \rangle = \langle i|k \rangle \langle j|l \rangle \pm \langle i|l \rangle \langle j|k \rangle \quad (20)$$

$$\begin{aligned} \langle \psi_p | \hat{H}_I | \psi_q \rangle &= \langle i|H_I|k \rangle \langle j|l \rangle \pm \langle i|H_I|l \rangle \langle j|k \rangle \\ &\quad + \langle j|H_I|l \rangle \langle i|k \rangle \pm \langle j|H_I|k \rangle \langle i|l \rangle \end{aligned} \quad (21)$$

$$\langle \psi_p | \hat{H}_{II} | \psi_q \rangle = \langle ij|H_{II}|kl \rangle \pm \langle ij|H_{II}|lk \rangle, \quad (22)$$

where $|ij\rangle := |i\rangle \otimes |j\rangle$ and where the sign ' \pm ' stands for '+' in the singlet case and for '-' in the triplet case.

All the $\frac{n(n+1)}{2}$ different one-particle matrix elements $\langle i|H_I|k \rangle$ are relatively easily evaluated (see Appendix B). Each matrix elements $\langle i|H_I|k \rangle$ equals a prefactor depending on the parameters of $|i\rangle$ and $|k\rangle$ times the one-particle overlap $\langle i|k \rangle$, reflecting the fact that the one-particle operators do not only conserve the total magnetic quantum number M and the total z -parity Π_z but also the magnetic quantum numbers and z -parities of the individual one-particle states. We remark that the mentioned prefactors in the matrix elements of the Zeeman term do not even depend on any basis state, rendering them purely proportional to the overlap, $\langle i|\frac{1}{2}\mathbf{B} \cdot \mathbf{l}|k \rangle = \frac{1}{2}m_k B \langle i|k \rangle$. Thus the Zeeman term just gives rise to a shift in the energies.

The only coupling between two-particle states composed of one-particle states with different combinations of magnetic quantum numbers or z -parities arises due to the two-particle operator of the electron-electron interaction. In contrast to the one-particle matrix elements the evaluation of the matrix elements $\langle ij|H_{II}|kl \rangle$ is by no means trivial (see Appendix C). An additional problem is the large number of different two-particle matrix elements which is of the order $\frac{N(N+1)}{2}$ rather than $\frac{n(n+1)}{2}$. This means that a sophisticated and detailed analysis of the analytical representation of the two-particle matrix elements by means of series of different representations of hypergeometric functions has been necessary in order to achieve an effective numerical implementation and an acceptable CPU time for performing a calculation for one given field strength. Details on the representation of the quantities $\langle ij|H_{II}|kl \rangle$ are given in Appendix C.

4 Results and discussion

4.1 Spectroscopic notation and properties

Before presenting the numerical results of our calculations we shall explain our spectroscopic notation in the presence of the field as well as its correspondence to the field-free notation. According to the four conserved quantities M , Π_z , \mathbf{S}^2 and S_z we denote a state by $\nu_{S_z}^{2S+1} M^{(-1)^{\Pi_z}}$ where $(2S+1)$ is the spin multiplicity and $\nu = 1, 2, 3, \dots$ is the degree of excitation within a given subspace. If obvious, we will omit the index S_z in the following. In the present paper we will investigate and show results for the subspaces $^10^+$, $^30^+$, $^10^-$, $^30^-$.

For vanishing field, there exists a one-to-one correspondence between our field notation and the common field-free notation $n_{S_z}^{2S+1}L_M$ (see Table 1). It is given by the fact that for bound helium eigenstates of \mathbf{L}^2 and L_z we have $(-1)^{\Pi_z} = (-1)^{L+M}$. The latter relation is not in general true for multi-electron systems because for a configuration containing two angular momenta l_1, l_2 we have $(-1)^{\Pi_z} = (-1)^{l_1+l_2+M}$. For helium and $B = 0$, however, all doubly excited states lie in the continuum[37] which means that all the helium states below the one-particle ionization threshold $T(B = 0) = -2.0a.u.$ must be one-particle excitations with $l_1 = 0$ and $l_2 = L$.

We emphasize that the mentioned one-to-one correspondence for $B = 0$ does not contradict the fact that the \mathbf{L}^2 -symmetry is higher than the Π_z -symmetry: At a finite field strength the former is broken whereas the latter is still valid. The field free notation becomes meaningless for finite field and could only be maintained as a labelling device for the energy eigenstates because a given $\nu_{S_z}^{2S+1}M^{(-1)^{\Pi_z}}$ state at a finite field develops in a unique way from the equally labelled $\nu_{S_z}^{2S+1}M^{(-1)^{\Pi_z}}$ state at $B = 0$ which, in turn, is identical with one unique $n_{S_z}^{2S+1}L_M$ state. We remark that energy curves within a subspace of given symmetries $\nu_{S_z}^{2S+1}M^{(-1)^{\Pi_z}}$ are not expected to cross [38], whereas crossings between curves of different subspaces are allowed.

In Table 1 we also provide the energies of the field free states which have been very precisely calculated by Accad et al. [30] or by Drake et al. [31]. We want to keep track of the energetical order of the states for several reasons. The first reason is that we need the energies for associating the energy quantum numbers ν to the states. It would not be sufficient to use the same counting n as in the field free case because there exist different states with the same n but different L which possess the same Π_z -symmetry, as is evident already for the states 3^10^+ and 4^10^+ .

The second reason is to point out the approximate degeneracy of the field free states with the same energy quantum number n but different L . Whereas the electron-electron interaction is only able to slightly perturb the otherwise exact degeneracy of those states, we will see that the magnetic field will completely remove this degeneracy. This effect can even be observed for the behaviour of the corresponding states in the H atom and thus is primarily an effect of the magnetic field alone rather than of the two-particle character of the He atom. It occurs in addition to the well-known removal of the degeneracy of states with the same quantum number L but different M whose energies split for finite field in $(2L + 1)$ different energy values.

The properties of the field free states of helium summarized in Table 1 serve as a good starting point for presenting our data for finite fields.

4.2 Aspects for the selection of basis functions

In order to obtain accurate results by our basis set method two major difficulties have been overcome by an optimal selection of basis functions. The first difficulty is the limited number n of one-particle functions from eq.(6) which can be used to describe the exact wave function. The second difficulty, which is not completely independent from the previous one, is to describe electronic correlation by using a basis composed of one-particle states.

One manifestation of correlation is the fact that different electrons avoid occupying the same region in space which we expect to be the consequence of the electron-electron repulsion as well in a magnetic field. In particular, we describe this by two electrons tending to occupy two regions in opposite directions from the nucleus which corresponds to the situation $\varphi_2 - \varphi_1 = \pi$. The Coulomb interaction $\frac{1}{|\mathbf{r}_1 - \mathbf{r}_2|}$ breaks the independent conservation of the z -components l_{z1}, l_{z2} of the two angular momenta, only leaving the sum $L_z = l_{z1} + l_{z2}$ as conserved quantity. A Fourier representation of the angular part of any fully correlated two-particle wave function $\Psi(\mathbf{r}_1, \mathbf{r}_2)$ is given by $\Psi(\varphi_1, \varphi_2) = \sum_{m_1, m_2} A_{m_1 m_2} e^{i(m_1 \varphi_1 + m_2 \varphi_2)}$. In order to obtain an eigenfunction of L_z we must demand the constraint $m_1 + m_2 = M$, yielding $\Psi(\varphi_1, \varphi_2) = e^{iM\varphi_1} \sum_m A_{M-m, m} e^{im(\varphi_2 - \varphi_1)}$. This expression contains angular correlation as can already be seen explicitly by considering the lowest

cosine term $B_m \cos m(\varphi_2 - \varphi_1)$ contained in the series above: assuming B_m to be negative, $\Psi(\varphi_1, \varphi_2)$ is largest for $\varphi_2 - \varphi_1 = \pi$ and lowest for $\varphi_2 - \varphi_1 = 0$. Therefore, it appears fruitful to choose one-particle wave functions with opposite magnetic quantum numbers ± 1 and ± 2 or even higher angular momenta combining to a total magnetic quantum number $M = 0$ in order to describe well the angular correlation. Correlation can also be described by wave functions possessing a node at the nucleus position and thus allowing the two electrons to be located in opposite directions with respect to the nucleus.

The maximum dimension N of the Hamiltonian matrix is limited by CPU and storage resources. Through a very efficient implementation (see appendices A,B,C) of the matrix elements and by optimized storage usage we were able to push the number of two-particle basis functions to $N \approx 4300$ which represents the limit with respect to linear dependencies of similar basis functions resulting in instabilities of the numerical diagonalisation of the generalized eigenvalue problem (11).

Let us discuss the strategy for the selection of basis functions for the example of the subspace 0^+ . We first focus on the basis functions optimized for a nuclear charge $Z = 1$, i.e. the hydrogen atom. We selected 31 functions with the symmetry 0^+ , among which 13 have a ρ -exponent equal 2 instead of 0 in order to describe correlation with the aid of their nodes. For further improving the description of correlation we used also each 13 functions with $m^{\pi z} = \pm 1^+$ and $m^{\pi z} = \pm 2^+$ as well as each 13 functions with $m^{\pi z} = 0^-$ and $m^{\pi z} = \pm 1^-$. The first excited state is already rather well described by this basis set but is still improved by adding basis functions optimized for excitations of the H atom in a magnetic field. Whereas for the first excited state correlation effects are still important the higher excitations are, like in the field free case, more and more dominated by one-electron excitations for which automatically the two electrons are spatially separated. Therefore, higher excitations were throughout described by adding functions with values $k_i = 1$ or $l_i = 1$ in eqs.(7) and (8) which are subsequently optimized to describe the corresponding higher excitations within the 0^+ subspace of hydrogen.

In order to describe higher excitations of the He atom the optimization for $Z = 1$ is sufficient because the nucleus with $Z = 2$ is screened by the inner electron. For the ground state and the first two excited states, however, we have observed important contributions also from functions optimized for $Z = 2$. Here we used a similar selection scheme as for the functions optimized for $Z = 1$, but only half the number of functions.

Altogether we arrive at a number of $n = 244$ different one-particle states, from which $N_1 = 4378$ two-particle states for singlet and $N_3 = 4288$ two-particle states for triplet spin symmetry can be composed according to eq.(15).

In a similar manner, we built up the basis for the 0^- subspace by involving functions optimized for $Z = 1$ as well as for $Z = 2$. We observe the effect of the latter optimized functions to be less significant in the 0^- case than in the 0^+ case. This appears natural since in any two-particle state with 0^- symmetry at least one electron is in an excited one-particle state and is only attracted by a screened nucleus with effective charge closer to $Z = 1$ than to $Z = 2$. Due to this reason we used altogether $n = 195$ one-particle states which is slightly less than in the 0^+ case. According to eq.(15) we obtain $N_1 = N_3 = 3600$ two-particle states for the singlet and triplet subspace, respectively. The numbers N_1 and N_3 do not differ due to the fact that the identical spatial one-particle quantum numbers which are always forbidden for the triplet two-particle states do not occur for the 0^- singlet subspace either because two different one-particle z -parities are required to form an odd total z -parity.

In the following subsection we discuss the results of our He calculations. Their accuracy is estimated by comparison with the field free data. If available, we provide also a comparison of our data for finite field strengths with the literature.

4.3 Energies for finite field strengths

4.3.1 Results for $M = 0$ and even z -parity

a) Results for the singlet states $\nu^1 0^+$

For the singlet subspace $\nu^1 0^+$ we present the ground state and the first four excitations, i.e. $1 \leq \nu \leq 5$. In the low-field and part of the intermediate regime the $1^1 0^+$ state is the global ground state. The numerical results for the total energy of the $1^1 0^+$ state as a function of the magnetic field are shown in Table 2. We observe that apart from $B = 0$ and $B = 0.08$ our results for the energies are throughout lower and thereby better than the best ones given in the literature. We remark that the $1^1 0^+$ state is the state which causes the most difficulties for an accurate description by our method. The first reason is that it is the only state for which both electrons considerably occupy the one-particle ground state which forces the two electrons to be close to each other in a narrow domain of space and which thus gives rise to a relatively strong contribution of electronic correlation. The second reason is that the mentioned one-particle ground state, which would be a Slater-type orbital for $B = 0$, possesses a cusp at the origin which is difficult to obtain accurately by a superposition of Gaussians. This second effect, however, can be expected to become less important with increasing field strength since the cusp in the direction perpendicular to the field axis is smoothed out by the increasing dominance of the magnetic field.

The overall increase of the total energies (see Table 2) with increasing field strength has its origin in the strongly increasing kinetic energy in the presence of the external field. The total binding energy of the two electrons can be obtained from the total energies $E(B)$ in Table 2 by subtracting the minimal energy B of two free electrons in the field, yielding $E(B) - B$ (here and in the following all ionizations are considered with fixed quantum numbers).

However, for an analysis of the electronic structure the one-electron ionization energies for the process $\text{He} \rightarrow \text{He}^+ + e^-$ are much more sensitive. The corresponding one-particle ionization threshold $T(B)$ is provided in the fourth column of Table 2. This threshold T can easily be obtained as the sum of the lowest Landau-energy $\frac{B}{2}$ of the ionized electron and the total one-particle energy $E_{\text{tot}}^{(1)}(Z = 2)$ of the other electron in the Coulomb field of the nucleus with charge $Z = 2$ in the presence of the magnetic field. This quantity $E_{\text{tot}}^{(1)}(Z = 2)$, in turn, can be received from the highly accurate values for the one-particle binding energy $E_{\text{bind}}^{(1)}(Z = 1)$ computed by Kravchenko et al. [5]. First we extract the total energies for $Z = 1$ from $(-E_{\text{bind}}^{(1)}(Z = 1)) := E_{\text{tot}}^{(1)}(Z = 1) - \frac{B}{2}$, and then we use the nuclear charge scaling relation $E(Z, B) = Z^2 E(Z = 1, B/Z^2)$ in ref.[6], yielding

$$T(B) = B - 4E_{\text{bind}}^{(1)}(Z = 1, B/4) \quad (23)$$

This threshold T lies essentially closer to the values $E(1^1 0^+)$ than the higher threshold B for two-particle ionization. We consider it in fact to be the optimal reference point for the total energies, and as expected the total energies of the excitations $\nu^1 0^+$ which are given in Table 3 approach closer and closer to the value T with increasing excitation. In agreement with the mentioned considerations about the special difficulties in achieving accurate results for the ground state we obtain much preciser values for the excitations within the same basis set.

The one-particle ionization energies for all the states $\nu^1 0^+$, $1 \leq \nu \leq 5$, i.e. the values of $E(B) - T(B)$, are given in Fig.1 as a function of the magnetic field. A logarithmic scale on the energy axis is necessary for covering the three orders of magnitude for the different states. We observe that though the ground state $1^1 0^+$ becomes monotonically stronger bound with increasing field strength this is not in general the case for the excitations. Below $B \sim 0.005 a.u.$ none of the energies differs considerably from its field free value. Between $B \sim 0.005 a.u.$ and $B \sim 0.1 a.u.$ a rearrangement takes place which is caused by the increasing

dominance of the magnetic forces over the Coulomb forces. The first effect to be observed is that the 4^10^+ state leaves the energetical vicinity of the 3^10^+ state. According to Table 1, for $B = 0$ these states would coincide with the states 3^1S_0 and 3^1D_0 , respectively, and thus both correspond to the same energy quantum number $n = 3$. The degeneracy of these two states is only slightly disturbed in the field-free case whereas a finite field removes this approximate degeneracy completely above $B \sim 0.01 a.u.$.

At $B \sim 0.08 a.u.$ the states 4^10^+ and 5^10^+ experience an avoided crossing. It can be recognized well even though the strong curvature of the graphs would make a finer grid of calculated energy values on the field axis desirable. The present grid is, nevertheless fine enough to observe that the calculated points are well aligned, confirming the good convergence of our calculations.

b) Results for the triplet states ν^30^+

For the triplet subspace ν^30^+ we present the ground state and the first three excitations, i.e. $1 \leq \nu \leq 4$. The numerical results together with the available data from the literature are given in Table 4. Much more data are available in the literature than for the singlet states. These numbers convincingly demonstrate that our approach to the solution of the two-electron problem in a strong magnetic field is superior to any other method existing in the literature.

Among the three related triplet states with $S_z = 0, \pm 1$ the one with $S_z = -1$ possesses the lowest energy due to the spin shift BS_z . Therefore, we have given in Table 4 those lowest energies. Although for $B = 0$ the singlet state 1^10^+ is the global ground state and the triplet state $1^3_00^+$ (i.e. $S_z = 0$) stays above it for any field strength, the spin shift ($-B$) causes the related triplet state $1^3_{-1}0^+(S_z = -1)$ to become the ground state within the $M = 0$ subspace above $B \sim 1.112 a.u.$. For the triplet ground state it is within our approach much easier to obtain accurate results than for the singlet ground state. This can be understood in the following picture: in the triplet ground state only one of the electrons occupies the one-particle ground state with the cusp whereas the other one occupies already predominantly an excited one-particle state and thus gives rise to a lower correlation contribution than in the singlet ground state.

In analogy to the case of the singlet states we provide in Fig.1 the dependence of the one-particle ionization energies on the field strength for the triplet states. The reference threshold $T(B)$ has the same value as for the singlet case because, following our general definition of the threshold, we keep the spins fixed.

We observe that the ionization energy of any state ν^30^+ in Fig.1 behaves similarly to the ionization energy of its singlet counterpart $(\nu + 1)^10^+$. This relationship has its origin in the fact that two states differing only with respect to their spin symmetry possess according to the field free notation in Table 1 similar contributions to their energies. The only difference with respect to the matrix elements of eqs.(20)-(22) for two such states is the sign of the exchange terms. Those might be small if the particles are sufficiently spatially separated as it is the case for all states apart from the 1^10^+ state. This statement is confirmed by the fact that the singlet-triplet splitting is particularly small between the 4^10^+ state and the 3^30^+ state. These states belong to the field free states 3^1D_0 and 3^3D_0 (see Table 1), respectively, and the one-particle orbitals with d -symmetry involved here are even more spatially separated from the participating s -orbitals than the p -orbitals playing a role in other states with larger singlet-triplet splitting. Of course this argumentation breaks down when the magnetic field destroys the spherical symmetry sufficiently and causes a mixture of total angular momenta. Consequently, the splitting between the 4^10^+ state and the 3^30^+ state grows considerably at $B \sim 0.02$.

4.3.2 Results for $M = 0$ and odd z -parity

a) Results for the singlet states ν^10^-

For the singlet subspace $\nu^1 0^-$ we present the ground state and the first four excitations, i.e. $1 \leq \nu \leq 5$. For $B \leq 0.08$, even the energies for the state $6^1 0^-$ show an excellent convergence. The corresponding data are presented in Table 5. For a graphical representation we choose the ionization energies which are calculated from the total energies with respect to the same threshold $T(B)$ as in the case of the 0^+ subspace. The reason is that in a one-electron ionization process of helium constrained to keep 0^- symmetry the ionized electron can adopt the negative z -parity, allowing the remaining electron to occupy the one-particle ground state which possesses 0^+ symmetry. The ionized electron, in turn, has the same Landau energy $\frac{B}{2}$ as in the 0^+ case because the z -parity does not have any influence on the Landau energy which is only assigned to the transversal degrees of freedom.

The curves for the ionization energies are shown in Fig.2. We observe that for very low fields the $6^1 0^-$ state and the $5^1 0^-$ state are approximately degenerate which is in agreement with the fact that for two values of ν, μ within the same bracket of the sequence (1), (2), (3, 4), (5, 6), (7, 8, 9), (10, 11, 12)... the two states $\nu^1 0^-$ and $\mu^1 0^-$ correspond to the same quantum number L according to Table 1. As in the 0^+ subspace, this approximate degeneracy is removed for fields above $B \sim 0.02$. The region between $B \sim 0.02$ and $B \sim 0.1$ exhibits some avoided crossings.

b) Results for the triplet states $\nu^3 0^-$

In contrast to the singlet case there exist much more data in the literature for the triplet state. In Table 6 we have listed them together with our results for the states $\nu_{-1}^3 0^-$ (i.e. $S_z = -1$), $1 \leq \nu \leq 5$. Again our results are better than any references for finite field strengths.

The ionization energies for the $\nu_{-1}^3 0^-$ states are also shown in Fig.2. As in the singlet case, we achieved a good convergence even for the fifth excited state $6^3 0^-$ below $B = 0.08$. The singlet-triplet splitting between the states $\nu^1 0^-$ and $\nu^3 0^-$ behaves similar as a function of the field like the corresponding splitting in the $1/3 0^+$ subspaces.

4.4 Transitions

In order to interpret experimental spectra from magnetic white dwarfs like GD229, it is necessary to determine transition energies from our total energies. The selection rules for electric dipole transitions are $\Delta S = 0$, $\Delta S_z = 0$ for the spin degrees of freedom and $\Delta M = 0$, $\Delta \Pi_z = \pm 1$ or $\Delta M = \pm 1$, $\Delta \Pi_z = 0$ for the spatial degrees of freedom. With the data presented we are able to treat the $\Delta M = 0$ transitions. We obtain a spectrum of 30 transition energy curves for singlet transitions and 24 ones for triplet transitions which we show in Fig.3a and 3b, respectively. In both logarithmic representations, we observe singularities belonging to zeros in the transition energies which arise due to level crossings of the initial state and the final state.

Since the magnetic field of a white dwarf is not constant but varies by a factor of two for a dipole geometry, the spectrum of wavelengths is in general smeared out. Transitions whose wavelengths are stationary with respect to the magnetic field, however, reflect themselves by characteristic absorption edges in the observable spectrum.

Due to this important role of the stationary lines we have summarized all transitions showing stationary points in Tables 7 and 8. The position and the wavelength of each stationary point have been determined by interpolation using the relatively crude grid of our calculations. This allows us to perform a comparison of the stationary components with the observed spectrum of the magnetic white dwarf GD229 [10]. Indeed, the accurate data on many excited states presented here are part of an analysis accomplished very recently [10] which clearly shows that there is strong evidence for the existence of He in the atmosphere of GD229. This might also be the case for other magnetic white dwarfs and therefore the present data will serve

astrophysicists for further comparison with observational data.

5 Conclusions and Outlook

We have investigated the electronic structure of the helium atom in a magnetic field by a fully correlated approach. We assumed the nucleus to possess infinite mass but provided scaling laws how to connect our fixed-nucleus results to the data which should be expected for the true finite nuclear mass. One of the goals of our work, the identification of the features in the spectrum of the white dwarf GD229 with electronic transitions in atomic helium, has already successfully been demonstrated[10]. This has been possible due to the high accuracy of our calculations on many excited states considering the electronic structure for magnetic fields for $0 \leq B \leq 100a.u.$, i.e. $0 \leq B \leq 2.3505 \cdot 10^7$ Tesla.

The starting point of our *ab initio* treatment of the helium atom in a magnetic field was its full fixed-nucleus Hamiltonian which possesses four conserved quantities: the total spin \mathbf{S}^2 and its z -component S_z , the z -component L_z of the electronic angular momentum and the electronic z -parity Π_z . Due to the magnetic field the spherical rotational invariance is broken resulting in the fact that the total electronic angular momentum \mathbf{L}^2 fails to be a conserved quantity for nonvanishing field $B \neq 0$. Our full configuration interaction approach has been able to overcome the difficulty that the symmetry of the system changes from purely spherical for $B = 0$ to mainly cylindrical for high fields. To this purpose we used a one-particle basis set of anisotropic Gaussians furnished with monomials in the coordinates ρ or z transversal or longitudinal to the field axis, respectively. The degree of anisotropy has been obtained as a result from the direct optimization of the nonlinear parameters for the transversal or longitudinal Gaussian by the requirement to solve optimally the one-particle problem of the H atom or the He^+ ion in a magnetic field of given strength. The one-particle basis functions were composed to two-particle states of pure total symmetry in the sense of the four conserved quantities mentioned above. In the present paper, we have provided results for the singlet and triplet states in the subspaces with vanishing spatial magnetic quantum number $M = 0$ and positive or negative z -parity.

In each of these subspaces we have built up a matrix for the Hamiltonian and for the overlap between the nonorthogonal two-particle states which provided a variational estimation for the energy eigenvalues after the diagonalization of a generalized eigenvalue problem. By very elaborate techniques for the evaluation of the matrix elements we were able to treat matrix dimensions of about 4000 within less than one day CPU time on a moderate Silicon Graphics workstation. The relative accuracy of the results for the energies ranged between 10^{-4} for the singlet ground states and 10^{-5} for the triplet states or general excited states for $2 < \nu < 5$. To achieve this, a careful selection of the basis functions was necessary, i.e. combinations of one-particle magnetic quantum numbers $m = \pm 1, \pm 2, \dots$ were important to describe correlation whereas one-particle functions describing high excitations of the one-particle systems H or He^+ provided the major contribution also for high excitations of the two-particle system He.

To enable a comparison of our calculated transitions with the observed spectra of magnetic white dwarfs, we have determined all the stationary points associated to the transitions between states with $M = 0$ and different z -parities. It turned out that the stationary points in the regime $B \sim 0.1$ and $B \sim 0.3$ can be identified with lines in the spectrum of the white dwarf GD229 which is even further confirmed by transitions involving $M = -1$ and positive z -parity[10, 41]. This provides strong evidence for the existence of helium in the atmosphere of this white dwarf. The present data will additionally be helpful in order to see whether there is evidence for helium also in other magnetic cosmic objects.

In order to complete the treatment of the electronic structure of helium in a magnetic field, we will in the near future calculate data for subspaces with higher magnetic quantum numbers for both odd and even

z -parity. Furthermore, a detailed investigation of the oscillator strengths as a function of the magnetic field is necessary in order to estimate properly the intensities of the transitions.

Acknowledgements. The Deutsche Studienstiftung (W.B.) and the Deutsche Forschungsgemeinschaft (W.B.) are gratefully acknowledged for financial support. P.S. acknowledges many helpful discussions during the CECAM workshop on 'Atoms in strong magnetic fields'. F.K.D. acknowledges financial support by the European Union. It is a pleasure for us to thank U. Kappes for many fruitful discussions as well as for his input with respect to the computational aspects of the present work.

A The overlap matrix elements

In the following we only give the results for the analytic representation of the matrix elements. The evaluation of the overlap integral is very simple because it factors into an integral over the transversal coordinate ρ and an integral over the longitudinal coordinate z . Both integrals can be reduced to a Gaussian type $\int_0^\infty t^n e^{-\gamma t^2} dt$, $n \geq 0$, yielding for the dependence of the one-particle overlap $\langle i|k \rangle$ on the parameters of the states $|i\rangle$ and $|k\rangle$:

$$\langle i|k \rangle = \delta_{m_i m_k} \delta_{\pi_{z_i} \pi_{z_k}} \cdot \pi^{\frac{3}{2}} \frac{(n_{z_{ik}} - 1)!! \left(\frac{n_{\rho_{ik}}}{2}\right)!}{2^{\frac{n_{z_{ik}}}{2}} \alpha_{ik}^{\frac{n_{\rho_{ik}}}{2} + 1} \beta_{ik}^{\frac{n_{z_{ik}} + 1}{2}}} \quad (24)$$

where we define $(-1)!! := 1$ and $\gamma_{ik} := \gamma_i + \gamma_k$. The Kronecker Delta symbols reflect the orthogonality of two one-particle states with different magnetic quantum numbers or different z -parities. We observe that the overlap is real and all the parameters of the wave functions $|i\rangle$ and $|k\rangle$ enter symmetrically in eq.(24).

B The one-particle matrix elements

B.1 The matrix elements of the kinetic energy

The matrix elements of the operator $(\mathbf{p} + \frac{1}{2}\mathbf{B} \times \mathbf{r})^2$ are evaluated by using cylindric coordinates in which we consider

$$\begin{aligned} (\mathbf{p} + \frac{1}{2}\mathbf{B} \times \mathbf{r})^2 &= -\frac{1}{2} \left(\left(\frac{\partial^2}{\partial \rho^2} + \frac{1}{\rho} \frac{\partial}{\partial \rho} \right) + \frac{1}{\rho^2} \frac{\partial^2}{\partial \varphi^2} + \frac{\partial^2}{\partial z^2} + iB \frac{\partial}{\partial \varphi} - \frac{1}{4} B^2 \rho^2 \right) \\ &=: (T_\rho + T_\varphi + T_z + T_{Zeeman} + T_{dia}) , \end{aligned} \quad (25)$$

where T_ρ, T_φ, T_z represent the Laplacian, T_{Zeeman} is the Zeeman term and T_{dia} the diamagnetic term. The evaluation of any of the matrix elements $\langle i|T_i|k \rangle$ is relatively simple since the derivatives generate prefactors but leave the types of the integrals unchanged in comparison to the overlap integral. A consequence is that the results are found to be proportional to the overlap $\langle i|k \rangle$ between the *same* two states. In detail we have

$$\langle i|T_\rho|k \rangle = \langle i|k \rangle \cdot \left\{ \begin{array}{ll} \frac{-n_{\rho_k}^2 \alpha_i^2 + 2(n_{\rho_i} n_{\rho_k} + n_{\rho_{ik}}) \alpha_i \alpha_k - n_{\rho_i}^2 \alpha_k^2}{n_{\rho_{ik}} \alpha_{ik}} & ; \ n_{\rho_{ik}} \neq 0 \\ \frac{2\alpha_i \alpha_k}{\alpha_{ik}} & ; \ n_{\rho_{ik}} = 0 \end{array} \right\} \quad (26)$$

$$\langle i|T_\varphi|k \rangle = \langle i|k \rangle \cdot \left\{ \begin{array}{ll} \frac{\alpha_{ik}}{n_{\rho_{ik}}} m_k^2 & ; \ n_{\rho_{ik}} \neq 0 \\ 0 & ; \ n_{\rho_{ik}} = 0 \end{array} \right\} \quad (27)$$

$$\langle i|T_z|k\rangle = \langle i|k\rangle \cdot \left\{ \frac{n_{zk}(1-n_{zk})\beta_i^2 + (2n_{zi}n_{zk} + n_{zik}-1)\beta_i\beta_k + n_{zi}(1-n_{zi})\beta_k^2}{(n_{zik}-1)\beta_{ik}} ; n_{zik} \neq 1 \right\} \quad (28)$$

$$\langle i|T_{Zeeman}|k\rangle = \langle i|k\rangle \cdot \frac{1}{2}m_k B \quad (29)$$

$$\langle i|T_{dia}|k\rangle = \langle i|k\rangle \cdot \frac{n_{\rho_{ik}} + 2}{2\alpha_{ik}} \cdot \frac{1}{8}B^2 \quad (30)$$

Again we observe that each matrix element is real and symmetric with respect to an interchange of the states $|i\rangle$ and $|k\rangle$. Due to the selection rules in the prefactor $\langle i|k\rangle$ the occurrence of the single quantity m_k does not destroy this symmetry. Physically, the proportionality to $\langle i|k\rangle$ means that the operator of the kinetic energy does not couple one-particle states involving different magnetic quantum number or z -parity.

B.2 The matrix elements of the electronic Coulomb interaction with the nucleus

The evaluation of the matrix elements of the one-particle operator $V_I = \frac{1}{r}$ is much more complicated than the other one-particle matrix elements discussed above. The reason is that the Coulomb potential possesses a spherical symmetry rather than the cylindrical symmetry of the basis functions. We have overcome this difficulty by applying a Singer transformation[42], leaving for the spacial integrations the convenient Gaussian types. The remaining integration due to the Singer transformation, however, is not as simple but it can be solved by involving the Gaussian hypergeometric function ${}_2F_1$, yielding

$$\langle i|V_I|k\rangle = -\langle i|k\rangle \cdot \beta_{ik}^{\frac{1}{2}} \frac{\Gamma\left(\frac{n_{\rho_{ik}} + n_{zik}}{2} + 1\right)}{\Gamma\left(\frac{n_{\rho_{ik}} + n_{zik}}{2} + \frac{3}{2}\right)} {}_2F_1\left(\frac{n_{\rho_{ik}}}{2} + 1, \frac{1}{2}, \frac{n_{\rho_{ik}} + n_{zik}}{2} + \frac{3}{2}; 1 - \frac{\beta_{ik}}{\alpha_{ik}}\right) \quad (31)$$

It is important to remark that very elaborate techniques are necessary to evaluate the function ${}_2F_1$ for the various occurring arguments with a high accuracy and with an acceptable efficiency. The standard expansion of ${}_2F_1(a, b, c; z)$ in a power series of z is by no means sufficient because a singularity of ${}_2F_1(a, b, c; z)$ for $z = 1$ constrains the convergence domain of such a series to $|z| < 1$. The consequence is that for $\frac{\beta_{ik}}{\alpha_{ik}} \ll 1$ the convergence of the standard series would be arbitrarily slow. Moreover, for $\frac{\beta_{ik}}{\alpha_{ik}} > 2$ the application of the standard series is completely useless. Using basis sets whose parameters α_i, β_i usually cover the range from 10^{-4} up to 10^5 , we have thus been obliged to use various formulas for suitable analytic continuations of ${}_2F_1(a, b, c; z)$ to the domain $|z| \geq 1$ [43]. By these techniques we achieved an accuracy of 10^{-13} for the one-particle interaction integrals with no loss of efficiency compared with the simple integrals of the kinetic energy.

We remark that also the matrix elements of the electron-nucleus interaction are proportional to the overlap $\langle i|k\rangle$. This is in agreement with the fact that the spherically symmetric Coulomb potential $V_I = \frac{1}{r}$ neither breaks the azimuthal symmetry nor disturbs the behaviour of the one-particle basis functions under the reflection $z \rightarrow -z$.

C The two-particle matrix elements

In contrast to the one-particle matrix elements treated above we cannot provide a single formula for the efficient and accurate calculation of the matrix elements $\langle ij|H_{II}|kl\rangle$ of the two-particle interaction. The reason is the large number of different cases due to the various constellations of the individual one-particle functions which have to be treated differently in order to ensure a fast and highly accurate evaluation. We therefore provide in the following only an outline of the procedure and indicate the necessary techniques. Details can be obtained from the authors upon request.

First we apply a Singer transformation[42] in order to remove the Coulomb singularity in the integrand of the matrix elements, thereby introducing the new variable u according to $\frac{1}{|\mathbf{r}_1 - \mathbf{r}_2|} = \frac{2}{\sqrt{\pi}} \int_0^\infty du e^{-u^2(\mathbf{r}_1 - \mathbf{r}_2)^2}$. Although the underlying symmetry of the basis set is cylindrical, it is advantageous to carry out the spatial integrations in Cartesian coordinates. The $z_1 z_2$ -integral can always be factored out, and the coupling between the two particles can be removed by the substitution $z_1 \rightarrow z_1 - \frac{u^2}{\beta_{ik} + u^2}$. The resulting integral can be decomposed into a sum of $(n_{zik} + 1)$ integrals each factoring in two pure z_1 and z_2 integrals of the Gaussian type $\int_{-\infty}^\infty z^n e^{-\beta(u)z^2}$ which can easily be evaluated.

The transversal part of the electron-electron integral is much more complicated than the z -integration. First each term $\rho_1^{|m_i|+|m_k|+2k_{ik}} e^{-i(m_i-m_k)\varphi_1}$ gives rise to factors $(k_{ik} + 1) \cdot (|m_i| + 1) \cdot (|m_k| + 1)$ according to its decomposition to $(x_1^2 + y_1^2)^{k_{ik}} (x_1 - i \operatorname{sgn}(m_i)y_1)^{|m_i|} (x_1 + i \operatorname{sgn}(m_k)y_1)^{|m_k|}$ in Cartesian coordinates (again the same number of expressions arises for particle 2). Next, the particle decoupling transformation analogous to the one mentioned above multiplies the number of integrals by an additional large factor n_d .

At this stage, all the Gaussian integrations in x_1, x_2, y_1, y_2, z_1 and z_2 can be carried out, resulting in functions of the remaining variable u of type $u^2(1 + a_1 u^2)^{r_1}(1 + a_2 u^2)^{r_2}(1 + a_3 u^2)^{r_3}(1 + a_4 u^2)^{r_4}$, where the r_i are positive or negative integers or half-integers. The coordinates can always be chosen such that one r_i is a positive integer. Multiplying out the factor $(1 + a_i u^2)^{r_i}$ enables us to reduce the remaining u -integral to an expression involving the Appell hypergeometric function $F_1(a, b, b', c; t_1, t_2)$.

For each of the $\frac{N(N+1)}{2}$ matrix elements $\langle ij|H_{II}|kl\rangle$, we thus have to evaluate $n_d \cdot \{(k_{ik} + 1) \cdot (|m_i| + 1) \cdot (|m_k| + 1)\}^2 \cdot (n_{zik} + 1) \cdot (r_i + 1)$ times the function F_1 with in general various different arguments a, b, b', c . Only the two arguments t_1, t_2 are universal for a fixed matrix element: $t_1 = \frac{\beta_{ik}}{\beta_{ik} + \beta_{jl}}$, and $t_2 = 1 - \frac{(\alpha_{ik} + \alpha_{jl})\beta_{ik}\beta_{jl}}{(\beta_{ik} + \beta_{jl})\alpha_{ik}\alpha_{jl}}$. For $|t_1| \ll 1$ and $|t_2| \ll 1$ we implemented the usual standard series expression of $F_1(a, b, b', c; t_1, t_2) = \sum_{m=0}^\infty \frac{(a, m)(b, m)}{(c, m)(1, m)} {}_2F_1(a + m, b'; c + m; t_2) t_1^m$, where ${}_2F_1(a, b; c; z) = \sum_{n=0}^\infty \frac{(a, n)(b, n)}{(c, n)(1, n)} z^n$ is the Gaussian hypergeometric function. However, the fact that for many basis functions either the argument $|t_1|$ or $|t_2|$ or even both happen to lie close to 1 or above makes this standard representation useless since its convergence domains are the unit circles with respect to t_1 and t_2 [44]. Therefore, it was necessary to use a large number of analytic continuation formulas for F_1 each of which is valid for one specified class of arguments a, b, b', c . Even more, we have systematically compared the CPU times for altogether more than 50 ways how to evaluate F_1 and selected the fastest one for each class of arguments, involving e.g. all of the continuation formulas for the Gaussian hypergeometric function ${}_2F_1(a, b, c; z)$ given in eqs.(15.3.3-15.3.12) in ref.[43]. We have additionally derived new formulas for ${}_2F_1(a, b, c; z)$ adapted for parameter constellations not covered in ref.[43], and we investigated the different possibilities how to reduce F_1 to ${}_2F_1$ or one of its derivatives.

We point out that without such a systematic analysis of the convergence properties of series representations for F_1 the present work would not have been possible: The reduction of CPU time for the same accuracy (10^{-12}) of our representation of the series compared to the most primitive selection of continuation formulas is about 10^3 .

References

- [1] H. Friedrich, Phys.Rev. **A 26**, 1827 (1982)
- [2] W. Rösner, G. Wunner, H. Herold and H. Ruder, J.Phys. **B 17**, 29 (1984)
- [3] D. Wintgen and H. Friedrich, J.Phys. **B 19**, 991 (1986)
- [4] M.V. Ivanov, J.Phys. **B 21**, 447 (1988)
- [5] Yu.P. Kravchenko, M.A. Liberman and B. Johansson, Phys.Rev. **A 54**, 287 (1996)
- [6] H. Ruder, G. Wunner, H. Herold und F. Geyer, Atoms in Strong Magnetic Fields, Springer Verlag A-A 1994.
- [7] P. Schmelcher and W. Schweizer, Atoms and Molecules in Strong External Fields, Plenum Press 1998
- [8] R.F. Green and J. Liebert, Pub. Astr. Soc. Pac 93, 105 (1980)
- [9] G.D. Schmidt et al. **ApJ** 350, 758 (1990)
- [10] S. Jordan, P. Schmelcher, W. Becken and W. Schweizer, Astronomy & Astrophysics Letters **336**, L33-L36 (1998)
- [11] G. Thurner, H. Herold, H. Ruder, G. Schlicht and G. Wunner, Phys. Letters, **89A**, no. 3, 133 (1982)
- [12] P. Pröschel, W. Rösner, G. Wunner, H. Ruder and H. Herold, J.Phys. **B 15**, 1959 (1982)
- [13] G. Thurner, H. Körbel, M. Braun, H. Herold, H. Ruder and G. Wunner, J.Phys. **B 26**, 4719 (1993)
- [14] M.V. Ivanov, Opt. Spectrosc. (USSR) **70** (2) (1991)
- [15] J. Virtamo, J.Phys. **B 9**, 751 (1976)
- [16] M.V. Ivanov, J.Phys. **B 27**, 4513 (1994)
- [17] M.D. Jones, G. Ortiz, D.M. Ceperley, Phys. Rev. **A 54**, 219 (1996)
- [18] R.O. Mueller, A.R.P. Rau and L. Spruch Phys. Rev. **A 11** 789 (1975)
- [19] M. Vincke and D. Baye, J. Phys **B 22** 2089 (1989)
- [20] D.M. Larsen, Phys.Rev. **B 20**, 20 (1979)
- [21] C.-H. Park and A.F. Starace, Phys.Rev. **A 29**, 442 (1984)
- [22] M.D. Jones, G. Ortiz, D.M. Ceperley, Phys.Rev. **E 55**, 6202 (1997)
- [23] M. Braun, W. Schweizer, H. Elster, Phys.Rev. **A 57**, 3739 (1998)
- [24] P. Schmelcher and L.S. Cederbaum, Phys.Rev. **A 37**, 672 (1988)
- [25] U. Kappes and P. Schmelcher, J.Chem.Phys. **100**, 2878 (1994); Phys.Rev. **A 51**, 4542 (1995); Phys.Rev. **A 53**, 3869 (1996)

- [26] T. Detmer, P. Schmelcher, F.K. Diakonov and L.S. Cederbaum, Phys.Rev. **A 56**, 1825 (1997)
- [27] T. Detmer, P. Schmelcher, L.S. Cederbaum, Phys.Rev. **A 57**, 1767 (1998)
- [28] A. Scrinzi, *private communications*
- [29] M. Braun, W. Schweizer and H. Herold, Phys.Rev.**A 48**, 1916 (1993)
- [30] Y. Accad and C.L. Pekeris, Phys.Rev. **A 24**, 516 (1971)
- [31] G.W.F. Drake and Z.-C. Yan, Phys.Rev. **A 46** 2378 (1992)
- [32] Z. Chen and S.P. Goldman, Phys. Rev. **A 45**, 1722 (1992)
- [33] V.B. Pavlov-Verevkin and B.I. Zhilinskii, Phys. Letters, **78A**, no. 3, 244 (1980)
- [34] B.R. Johnson, J.O. Hirschfelder and K.-H. Yang, Reviews of Modern Physics **55**, 109 (1983)
- [35] P. Schmelcher, L.S. Cederbaum and U. Kappes, Conceptual Trends in Quantum Chemistry, Kluwer Academic Publisher 1994, p.1-51
- [36] P. Schmelcher and L.S. Cederbaum, Phys.Rev. **A 43**, 287 (1991)
- [37] W.B. Westerveld, F.B. Kets, H.G.M. Heideman and J. van Eck, J.Phys. **B 12** 15 2575 (1979)
- [38] J. von Neumann und E.P. Wigner, Eigenwerte bei adiabatischen Prozessen, Physik. Zeitschrift. **XXX**, 467 (1929)
- [39] J.D. Baker, D.E. Freund, R.N. Hill and J.D. Morgan III, Phys. Rev.**A 41**, 1247 (1990)
- [40] J.D. Baker, R.N. Hill and J.D. Morgan III, in *Relativistic, Quantum Electrodynamical, and Weak Interaction Effects in Atoms*, edited by Walter Johnson, Peter Mohr, and Joseph Sucher, AIP Conf. Proc. No. 189 (American Institute of Physics, New York, 1989), pp. 123-145.
- [41] W. Becken and P. Schmelcher, *in preparation*
- [42] K. Singer, Proc. R. Soc. Lond. **A 402**, 412 (1960)
- [43] M. Abramowitz and I.A. Stegun, Handbook of mathematical functions, Dover Publications, 1972
- [44] Appell et Kampé de Fériet, Les fonctions hypergéométriques et hypersphériques, Gauthier-Villars et Cie, Editeurs, Paris 1926

Fig.1

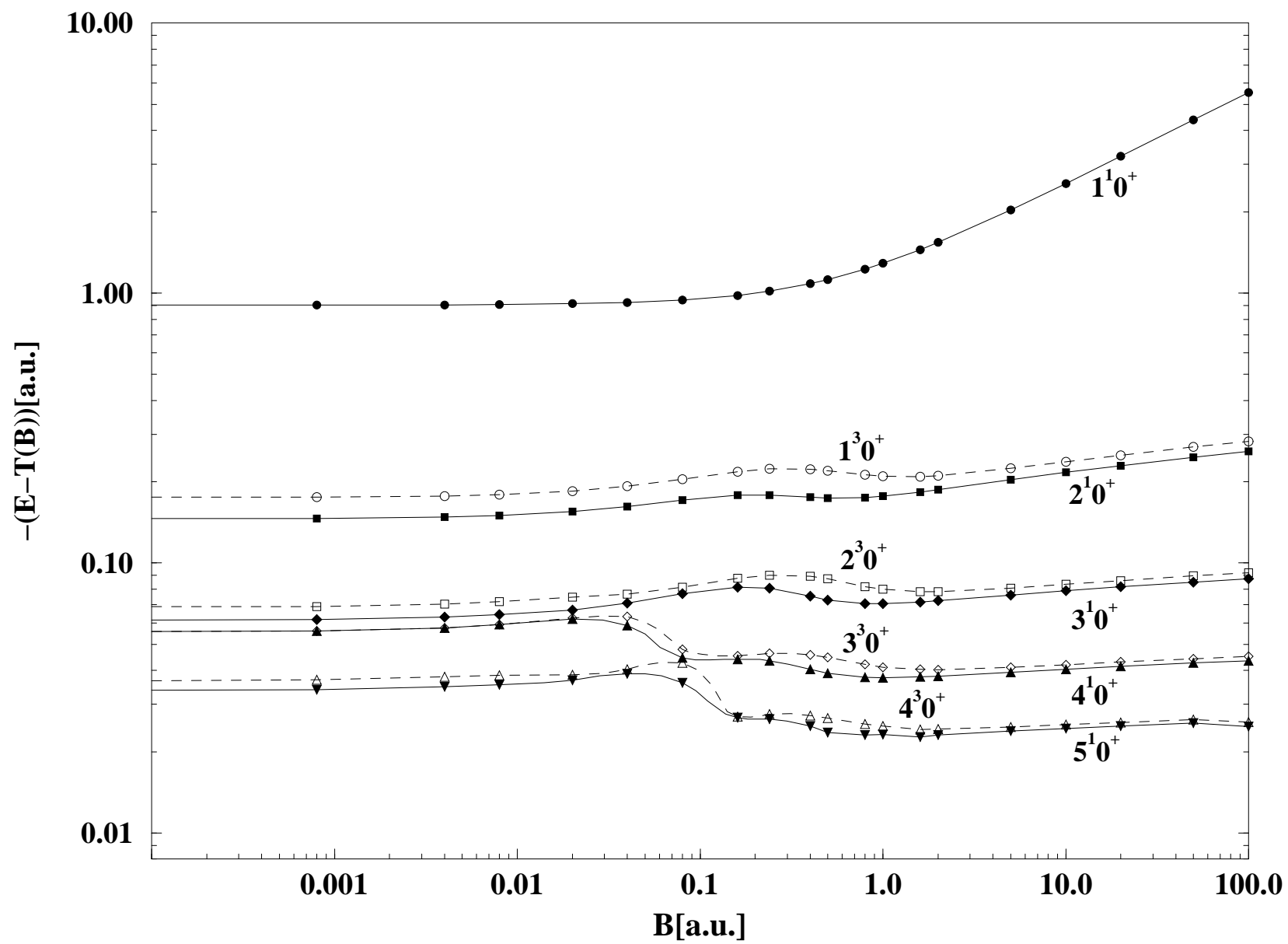


Fig.2

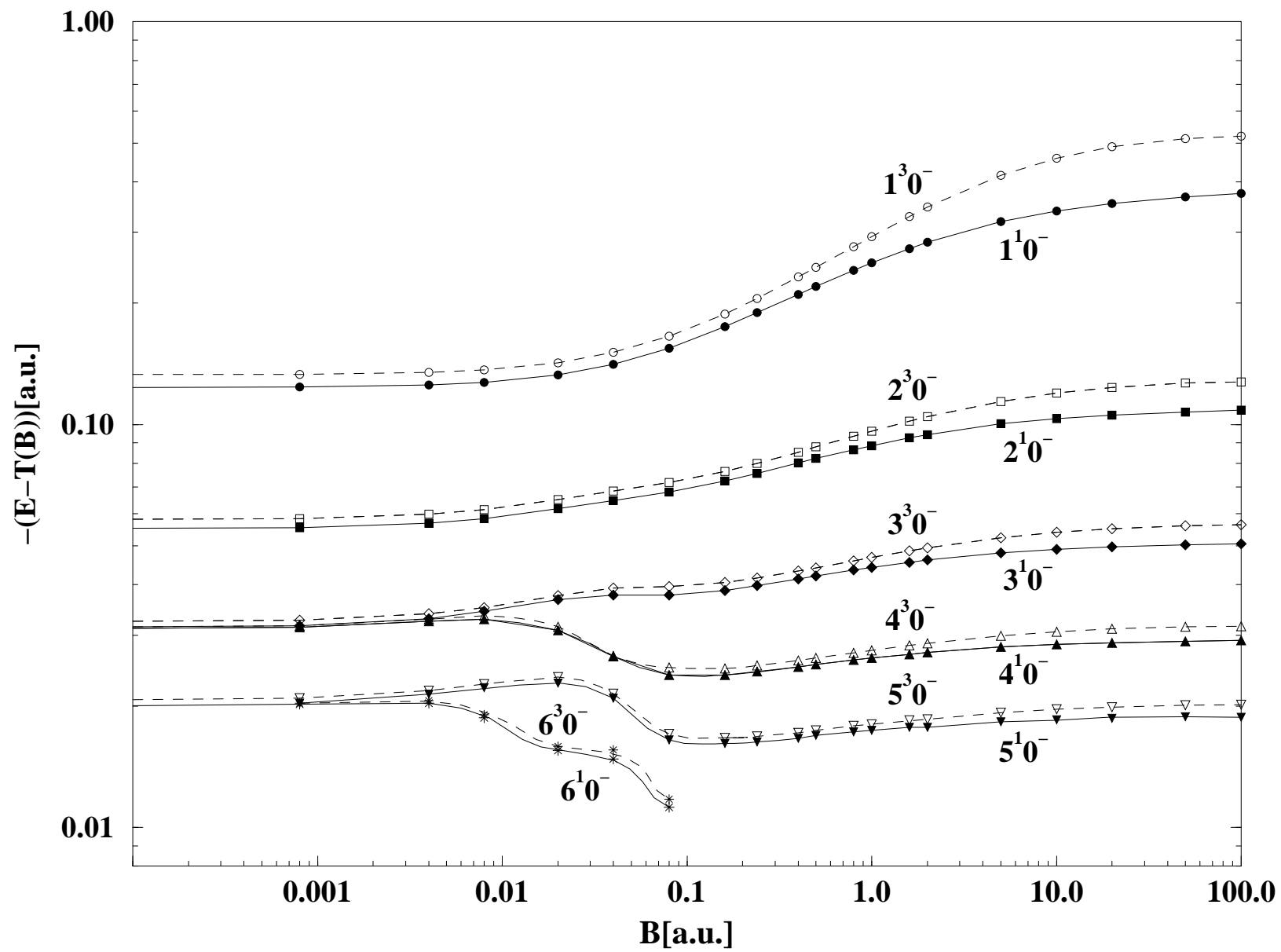


Fig.3a

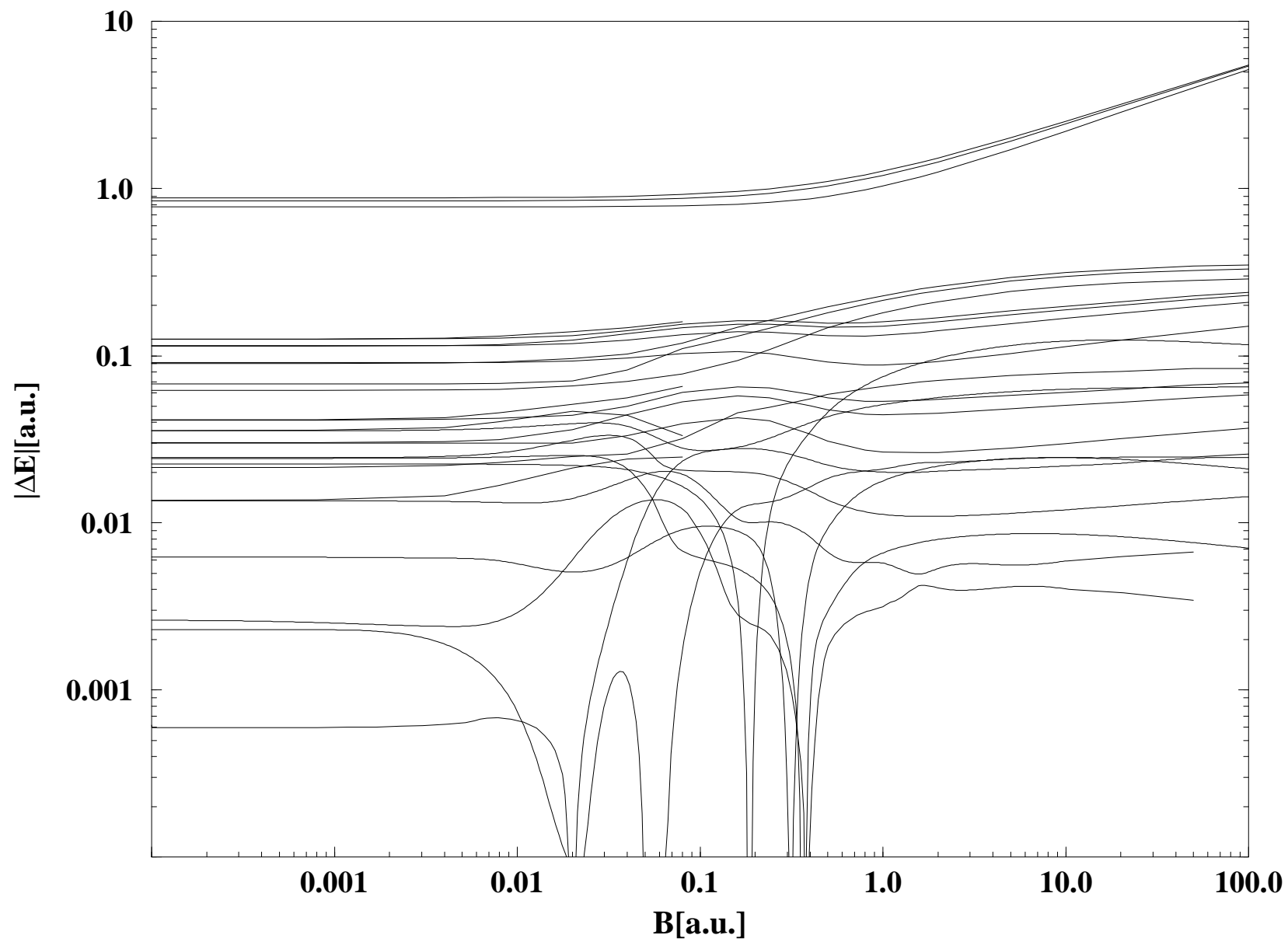


Fig.3b

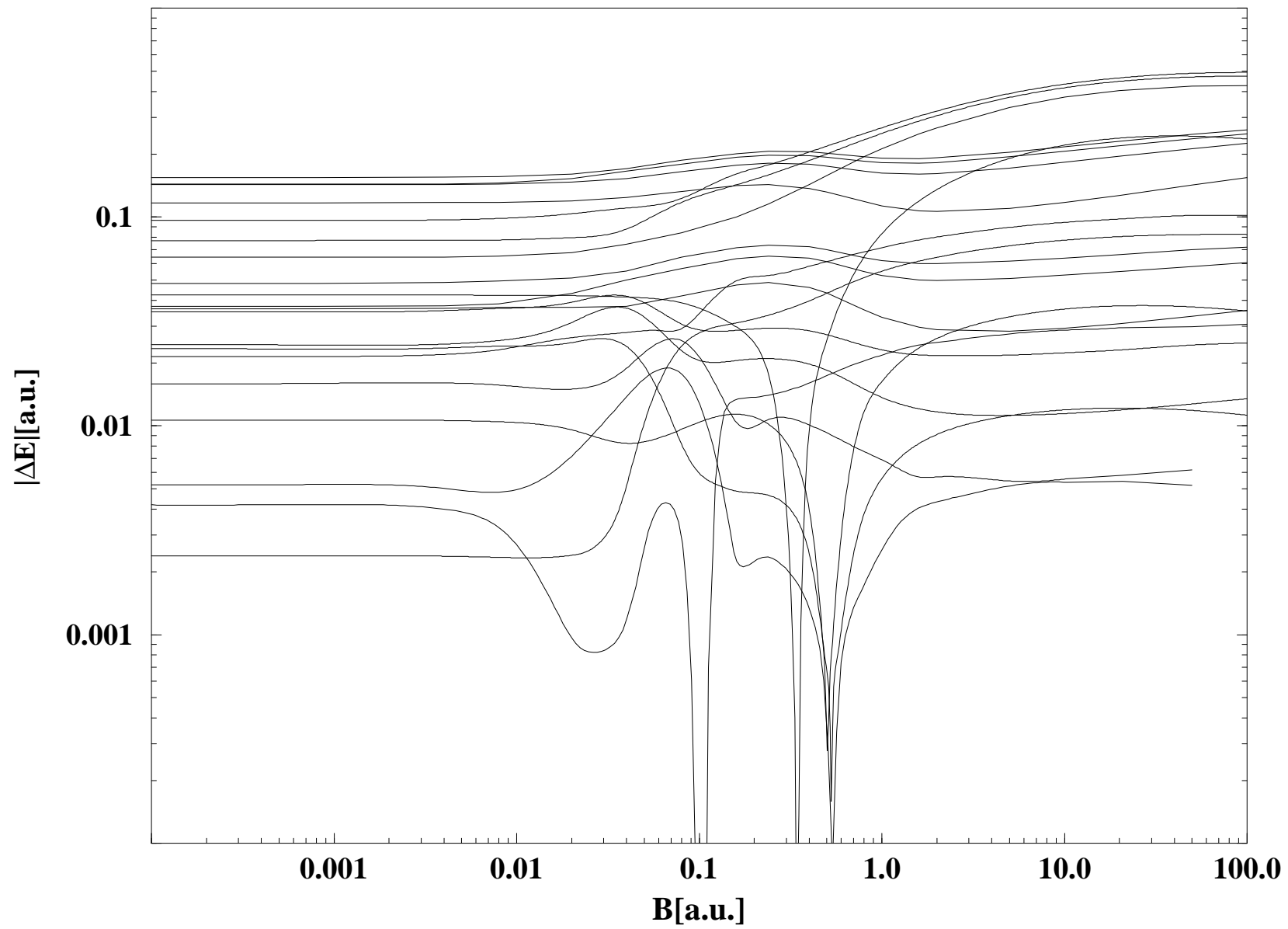


Figure Captions

Fig.1. Ionization energies of the singlet and triplet states k^10^+ and n^30^+ , $k = 1, \dots, 5$, $n = 1, \dots, 4$. The solid lines correspond to the singlet states, the dashed ones show the triplet states. Apart from the state 1^10^+ every singlet state possesses a triplet counterpart which is separated only by a small singlet-triplet splitting.

Fig.2. Ionization energies of the singlet and triplet states k^10^- and n^30^- , $k = 1, \dots, 6$, $n = 1, \dots, 6$. The solid lines correspond to the singlet states, the dashed ones show the triplet states.

Fig.3 (a) Transition energies for the singlet transitions $\mu^10^+ \rightarrow \nu^10^-$, $\mu = 1, \dots, 5$, $n = 1, \dots, 6$ as a function of the field strength. The curves are interpolated on a grid of field strengths given by our calculations.
 (b) Transition energies for the triplet transitions $\mu^30^+ \rightarrow \nu^30^-$, $\mu = 1, \dots, 4$, $n = 1, \dots, 6$ as a function of the field strength.

Tables

Table 1: Correspondence table between the field notation $\nu^{2S+1}M^{(-1)^{\Pi_z}}$ and the familiar field free notation $n^{2S+1}L_M$ for the lowest 55 singlet states and the lowest 54 triplet states of He. We have also provided the precise total zero-field energy of each state given in the literature.

field free		field
Energy	$n^{2S+1}L_M$	$\nu^{2S+1}M^{(-1)^{\Pi_z}}$
-2.903724377 ^a	1^1S_0	1^10^+
-2.145974046 ^a	2^1S_0	2^10^+
-2.1238430864 ^b	2^1P_0	1^10^-
	$2^1P_{\pm 1}$	$1^1(\pm 1)^+$
-2.061271988 ^a	3^1S_0	3^10^+
-2.0556207328 ^b	3^1D_0	4^10^+
	$3^1D_{\pm 1}$	$1^1(\pm 1)^-$
	$3^1D_{\pm 2}$	$1^1(\pm 2)^+$
-2.0551463620 ^b	3^1P_0	2^10^-
	$3^1P_{\pm 1}$	$2^1(\pm 1)^+$
-2.033586717 ^a	4^1S_0	5^10^+
-2.0312798461 ^b	4^1D_0	6^10^+
	$4^1D_{\pm 1}$	$2^1(\pm 1)^-$
	$4^1D_{\pm 2}$	$2^1(\pm 2)^+$
-2.0312551443 ^b	4^1F_0	3^10^-
	$4^1F_{\pm 1}$	$3^1(\pm 1)^+$
	$4^1F_{\pm 2}$	$1^1(\pm 2)^-$
	$4^1F_{\pm 3}$	$1^1(\pm 3)^+$
-2.0310696504 ^b	4^1P_0	4^10^-
	$4^1P_{\pm 1}$	$4^1(\pm 1)^+$
-2.0211137 ^c	5^1S_0	7^10^+
-2.0200158361 ^b	5^1D_0	8^10^+
	$5^1D_{\pm 1}$	$3^1(\pm 1)^-$
	$5^1D_{\pm 2}$	$3^1(\pm 2)^+$
-2.0200029371 ^b	5^1F_0	5^10^-
	$5^1F_{\pm 1}$	$5^1(\pm 1)^+$
	$5^1F_{\pm 2}$	$2^1(\pm 2)^-$
	$5^1F_{\pm 3}$	$2^1(\pm 3)^+$
-2.0200007108 ^b	5^1G_0	9^10^+
	$5^1G_{\pm 1}$	$4^1(\pm 1)^-$
	$5^1G_{\pm 2}$	$4^1(\pm 2)^+$
	$5^1G_{\pm 3}$	$1^1(\pm 3)^-$
	$5^1G_{\pm 4}$	$1^1(\pm 4)^+$
-2.0199059899 ^b	5^1P_0	6^10^-
	$5^1P_{\pm 1}$	$6^1(\pm 1)^+$

field free		field
Energy	$n^{2S+1}L_M$	$\nu^{2S+1}M^{(-1)^{\Pi_z}}$
—	—	—
-2.175229378 ^a	2^3S_0	1^30^+
-2.133164191 ^b	2^3P_0	1^30^-
	$2^3P_{\pm 1}$	$1^3(\pm 1)^+$
-2.068689067 ^a	3^3S_0	2^30^+
-2.058081084 ^b	3^3P_0	2^30^-
	$3^3P_{\pm 1}$	$2^3(\pm 1)^+$
-2.055636309 ^b	3^3D_0	3^30^+
	$3^3D_{\pm 1}$	$1^3(\pm 1)^-$
	$3^3D_{\pm 2}$	$1^3(\pm 2)^+$
-2.036512083 ^a	4^3S_0	4^30^+
-2.032324354 ^b	4^3P_0	3^30^-
	$4^3P_{\pm 1}$	$3^3(\pm 1)^+$
-2.031288847 ^b	4^3D_0	5^30^+
	$4^3D_{\pm 1}$	$2^3(\pm 1)^-$
	$4^3D_{\pm 2}$	$2^3(\pm 2)^+$
-2.031255168 ^b	4^3F_0	4^30^-
	$4^3F_{\pm 1}$	$4^3(\pm 1)^+$
	$4^3F_{\pm 2}$	$1^3(\pm 2)^-$
	$4^3F_{\pm 3}$	$1^3(\pm 3)^+$
-2.02261624 ^c	5^3S_0	6^30^+
-2.020551187 ^b	5^3P_0	5^30^-
	$5^3P_{\pm 1}$	$5^3(\pm 1)^+$
-2.020021027 ^b	5^3D_0	7^30^+
	$5^3D_{\pm 1}$	$3^3(\pm 1)^-$
	$5^3D_{\pm 2}$	$3^3(\pm 2)^+$
-2.020002957 ^b	5^3F_0	6^30^-
	$5^3F_{\pm 1}$	$6^3(\pm 1)^+$
	$5^3F_{\pm 2}$	$2^3(\pm 2)^-$
	$5^3F_{\pm 3}$	$2^3(\pm 3)^+$
-2.020000711 ^b	5^3G_0	8^30^+
	$5^3G_{\pm 1}$	$4^3(\pm 1)^-$
	$5^3G_{\pm 2}$	$4^3(\pm 2)^+$
	$5^3G_{\pm 3}$	$1^3(\pm 3)^-$
	$5^3G_{\pm 4}$	$1^3(\pm 4)^+$

^a Baker et al. (1990) [39]

^b Drake et al. (1992) [31]

^c Accad et al. (1971) [30]

Table 2: Total energies E of the singlet ground state 1^10^+ , one-electron ionization threshold T and, if available, best energy values given in the literature, as a function of the magnetic field strength B

B	$E(1^10^+)$	literature	T
0.0000	-2.903351	-2.903724377^a	-2.000
0.0008	-2.903346		-1.999599960
0.004	-2.903342		-1.997999000
0.008	-2.903340		-1.995995995
0.020	-2.903270		-1.989975001
0.040	-2.903036		-1.979900008
0.080	-2.902083	-2.90195^d	-1.959600176
0.160	-2.898290		-1.918402804
0.240	-2.892035		-1.876414090
0.400	-2.872501		-1.790105922
0.500	-2.855859	-2.85385^e	-1.734628064
0.800	-2.787556	-2.77585^d	-1.561526260
1.000	-2.729508	-2.7272^e	-1.440989741
1.600	-2.507952	-2.3266^e	-1.058421519
2.000	-2.329780		-0.788842154
5.000	-0.574877		1.456132354
10.000	3.064582		5.609851957
20.000	11.267051		14.47840453
50.000	38.076320		42.45369755
100.000	84.918313		90.43945348

^a Baker et al. (1990) [39]

^d Thurner et al. (1982) [11]

^e Larsen (1979) [20]

Table 3: Total energies E of the excited singlet states $\nu^1 0^+$ for $2 \leq \nu \leq 5$ as a function of the magnetic field strength B as well as field free reference values

B	$E(2^1 0^+)$	$E(3^1 0^+)$	$E(4^1 0^+)$	$E(5^1 0^+)$
0.0000	-2.145912	-2.061255	-2.055613	-2.033579
0.0000 (lit.)	-2.145974046 ^a	-2.061271988 ^a	-2.055620732852245 ^b	-2.033586717026 ^a
0.0008	-2.145911	-2.061246	-2.055607	-2.033531
0.004	-2.145869	-2.061028	-2.055489	-2.032867
0.008	-2.145743	-2.060374	-2.055122	-2.031451
0.020	-2.144852	-2.056838	-2.052030	-2.026808
0.040	-2.141787	-2.050850	-2.038691	-2.018836
0.080	-2.130812	-2.036626	-2.004123	-1.995610
0.160	-2.096743	-1.999728	-1.962448	-1.945128
0.240	-2.054961	-1.956971	-1.919910	-1.902875
0.400	-1.965307	-1.865411	-1.830581	-1.814978
0.500	-1.908671	-1.807640	-1.773700	-1.758191
0.800	-1.736422	-1.632339	-1.599198	-1.584566
1.000	-1.617870	-1.511771	-1.478551	-1.464143
1.600	-1.241729	-1.130213	-1.096276	-1.081100
2.000	-0.975861	-0.861382	-0.826959	-0.811912
5.000	1.252363	1.379993	1.416706	1.432270
10.000	5.393200	5.530945	5.569418	5.585430
20.000	14.248991	14.396817	14.437004	14.453455
50.000	42.207510	42.368689	42.411075	42.428159
100.000	90.180690	90.351969	90.395965	90.414700

^a Baker et al. (1989) [40]

^b Drake et al. (1992) [31]

Table 4: Total energies E of the triplet states $\nu_{-1}^3 0^+$ ($S_z = -1$) for $1 \leq \nu \leq 4$ as a function of the magnetic field strength B . We have also provided the results given in the literature so far.

	$E(1^3 0^+)$		$E(2^3 0^+)$		$E(3^3 0^+)$		$E(4^3 0^+)$	
B	this work	literature	this work	literature	this work	lit.	this work	literature
0.0000	-2.175220	-2.175229 378 ^a	-2.068687	-2.068689 067472 ^a	-2.055630	-2.055636309453 ^b	-2.036511	-2.036512 083098 ^a
0.0008	-2.176019	-2.175050 ^f	-2.069480	-2.069278 ⁱ	-2.056424		-2.037278	
0.004	-2.179190	-2.178220 ^f	-2.072505	-2.072302 ⁱ	-2.059507		-2.039893	
0.008	-2.183098	-2.1830(5) ^g	-2.075969	-2.0760(1) ^g	-2.063153		-2.042333	-2.0413(4) ^g
0.020	-2.194461		-2.084626		-2.072654		-2.048567	
0.040	-2.212236	-2.211222 ^f	-2.096580	-2.092686 ⁱ	-2.083143		-2.060290	
0.080	-2.243958	-2.2438(3) ^g	-2.121107	-2.1209(1) ^g	-2.087409		-2.082249	-2.0687(9) ^g
0.160	-2.296318		-2.166290		-2.123762		-2.105446	
0.240	-2.339560		-2.206689	-2.1927 ^f	-2.162609		-2.143909	
0.400	-2.412723	-2.4112 ^f	-2.279523	-2.2615 ^f	-2.235815		-2.217383	
0.500	-2.454347	-2.4528 ^h	-2.321985		-2.279382		-2.261303	
0.800	-2.573615	-2.5737(3) ^g	-2.443352	-2.4395(9) ^g	-2.403631		-2.386891	-2.3497(21) ^g
1.000	-2.650655	-2.6492 ^h	-2.520902		-2.482164		-2.465921	
1.600	-2.867620	-2.8669(5) ^g	-2.736687	-2.7330(8) ^g	-2.698755		-2.682563	-2.6665(26) ^g
2.000	-2.999708	-2.9982 ^h	-2.867135		-2.829137		-2.813101	
5.000	-3.768199	-3.7667 ^h	-3.624558		-3.584967		-3.568584	
10.000	-4.627450	-4.626 ^h	-4.473459		-4.432177		-4.415350	
20.000	-5.772448	-5.771 ^h	-5.607619		-5.564582		-5.547290	
50.000	-7.815256	-7.814 ^h	-7.635847		-7.590520		-7.563695	
100.00	-9.843074	-9.842 ^h	-9.652632		-9.605634		-9.586289	

^a Baker et al. (1989) [40]

^b Drake et al. (1992) [31]

^f Jones et al. (1996) [17]

^g Jones et al. (1997) [22]

^h Ivanov (1994) [16]

ⁱ Thurner et al. (1993) [13]

Table 5: Total energies E of the states $\nu^1 0^-$, $1 \leq \nu \leq 6$ as a function of the magnetic field strength B as well as field free reference values and the values for finite field, if available. For $B > 0.1$ a.u., the energy values for the $6^1 0^-$ state are not optimally converged

B	$E(1^1 0^-)$	$E(2^1 0^-)$	$E(3^1 0^-)$	$E(4^1 0^-)$	$E(5^1 0^-)$	$E(6^1 0^-)$
0.0000	-2.123412	-2.055015	-2.031252	-2.031014	-2.019999	-2.019877
	-2.123843430864 ^b	-2.0551463620 ^b	-2.0312551443 ^b	-2.03106965 ^b	-2.020002937 ^b	-2.019905990 ^b
0.0008	-2.123413	-2.055009	-2.031238	-2.030994	-2.019958	-2.019824
0.004	-2.123388	-2.054868	-2.030983	-2.030463	-2.019427	-2.018337
0.008	-2.123314	-2.054438	-2.030349	-2.028842	-2.018198	-2.014716
0.020	-2.122782	-2.051758	-2.026727	-2.020802	-2.012781	-2.005504
0.040	-2.120940	-2.044641	-2.017663	-2.006440	-2.000816	-1.994681
0.080	-2.114310	-2.027515	-1.997336	-1.983478	-1.976059	-1.970825
0.160	-2.093203	-1.990787	-1.957118	-1.942289	-1.934541	
0.240	-2.065812	-1.952090	-1.916192	-1.900745	-1.892719	
0.400	-2.000350	-1.870342	-1.831436	-1.815130	-1.806747	
0.500	-1.954646	-1.816921	-1.776662	-1.759971	-1.751519	
	-1.95455 ^e					
0.800	-1.802966	-1.648143	-1.605029	-1.587531	-1.578773	
1.000	-1.692794	-1.529609	-1.485166	-1.467297	-1.458395	
	-1.69185 ^e					
1.600	-1.331851	-1.151043	-1.103929	-1.085324	-1.076152	
2.000	-1.072194	-0.883229	-0.834929	-0.816003	-0.806576	
	-1.06905 ^e					
5.000	1.137045	1.355762	1.408108	1.428117	1.437859	
10.000	5.270657	5.506354	5.560836	5.581403	5.591347	
20.000	14.124717	14.372781	14.428726	14.449668	14.459766	
50.000	42.086569	42.346227	42.403449	42.424712	42.434863	
100.000	90.064304	90.330942	90.388895	90.410339	90.420669	

^b Drake et al. (1992) [31]

^e Larsen (1979) [20]

Table 6: Total energies E of the triplet states $\nu_{-1}^3 0^-$ ($S_z = -1$) for $1 \leq \nu \leq 6$ as a function of the magnetic field strength B . We have also provided the results given in the literature so far.

	$E(1^3 0^-)$		$E(2^3 0^-)$		$E(3^3 0^-)$		$E(4^3 0^-)$		$E(5^3 0^-)$		$E(6^3 0^-)$	
B	this work	literature	this work	literature	this work	literature	this work	lt.	this work	lt.	this work	lt.
0.0000	-2.132910	-2.133164 191 ^b	-2.058016	-2.058081 084 ^b	-2.032298	-2.032324 354 ^b	-2.031252	-2.031255168 ^b	-2.020538	-2.020551187 ^b	-2.020002957 ^b	
0.0008	-2.133710	-2.1323 ^f	-2.058810	-2.0584 ^f	-2.033081		-2.032038		-2.021293		-2.020753	
0.004	-2.136889	-2.1344 ^f	-2.061884	-2.0615 ^f	-2.035896		-2.034870		-2.023839		-2.022647	
0.008	-2.140826	-2.1408(8) ^g	-2.065499	-2.0655(5) ^g	-2.039077	-2.0350(10) ^g	-2.037514		-2.026642		-2.023039	
0.020	-2.152378		-2.075054		-2.047603		-2.041411		-2.033564		-2.025840	
0.040	-2.170822	-2.169276 ⁱ	-2.088326	-2.086102 ⁱ	-2.059120		-2.046510		-2.041394		-2.035472	
0.080	-2.205130	-2.2050(6) ^g	-2.111478	-2.1100(3) ^g	-2.079242	-2.0578(14) ^g	-2.064505		-2.056648		-2.051347	
0.160	-2.266575	-2.262806 ⁱ	-2.154912	-2.112992 ⁱ	-2.118891		-2.103193		-2.095063			
0.240	-2.322032	-2.3198 ^f	-2.196517	-2.1868 ^f	-2.157959		-2.141609		-2.133225			
0.400	-2.422361	-2.4196 ^f	-2.275521	-2.2463 ^f	-2.233362		-2.216039		-2.207275			
0.500	-2.480172		-2.322570		-2.278711		-2.260925		-2.252044			
0.800	-2.638222	-2.6397(9) ^g	-2.455054	-2.4545(6) ^g	-2.407425	-2.3925(7) ^g	-2.388624		-2.379366			
1.000	-2.733813		-2.537231		-2.487761		-2.468471		-2.459030			
1.600	-2.987185	-2.9873(8) ^g	-2.760330	-2.7596(8) ^g	-2.706990	-2.6749(6) ^g	-2.686687		-2.676877			
2.000	-3.135142		-2.893357		-2.838224		-2.817461		-2.807405			
5.000	-3.959235		-3.657879		-3.596162		-3.573739		-3.563137			
10.000	-4.848590		-4.509715		-4.444111		-4.420729		-4.409789			
20.000	-6.011488		-5.645191		-5.576755		-5.552682		-5.541487			
50.000	-8.059466		-7.672999		-7.602384		-7.577781		-7.566423			
100.00	-10.079973		-9.688173		-9.616899		-9.592135		-9.580675			

^b Drake et al. (1992) [31]

^f Jones et al. (1996) [17]

^g Jones et al. (1997) [22]

ⁱ Thurner et al. (1993) [13]

Table 7: Overview over all of the stationary points found in of the singlet transitions $\mu^1 0^+ \rightarrow \nu^1 0^-$ for $\mu = 1, \dots, 5$, $\nu = 1, \dots, 5$ in the range $0 \leq B \leq 100 a.u.$. The main part of the errors arises due to the interpolation over the relatively crude grid of field strengths. For high wavelengths, the finite accuracy of the energy values themselves contributes also to error in the energies.

Component $\nu^{2S+1}M^{(-1)^{\Pi_z}}$	wavelength/A	position $B/a.u.$	max/min
$2^1 0^+ \rightarrow 1^1 0^-$	3665 ± 13	18.3 ± 0.3	min
$2^1 0^+ \rightarrow 2^1 0^-$	4291 ± 5	0.140 ± 0.005	min
$2^1 0^+ \rightarrow 2^1 0^-$	5169 ± 11	0.899 ± 0.003	max
$2^1 0^+ \rightarrow 3^1 0^-$	3258 ± 5	0.184 ± 0.005	min
$2^1 0^+ \rightarrow 3^1 0^-$	3475 ± 6	0.68 ± 0.02	max
$2^1 0^+ \rightarrow 4^1 0^-$	2949 ± 10	0.17 ± 0.02	min
$2^1 0^+ \rightarrow 4^1 0^-$	3073 ± 5	0.625 ± 0.005	max
$2^1 0^+ \rightarrow 5^1 0^-$	2797 ± 5	0.200 ± 0.005	min
$2^1 0^+ \rightarrow 5^1 0^-$	2905 ± 5	0.605 ± 0.005	max
$3^1 0^+ \rightarrow 2^1 0^-$	90300 ± 3000	0.023 ± 0.001	max
$3^1 0^+ \rightarrow 2^1 0^-$	43600 ± 1000	0.11 ± 0.02	min
$3^1 0^+ \rightarrow 2^1 0^-$	18518 ± 100	8.9 ± 0.2	min
$3^1 0^+ \rightarrow 3^1 0^-$	10655 ± 40	0.14 ± 0.01	min
$3^1 0^+ \rightarrow 3^1 0^-$	17350 ± 40	1.45 ± 0.1	max
$3^1 0^+ \rightarrow 4^1 0^-$	7916 ± 40	0.18 ± 0.01	min
$3^1 0^+ \rightarrow 4^1 0^-$	10250 ± 10	1.05 ± 0.10	max
$3^1 0^+ \rightarrow 5^1 0^-$	6969 ± 40	0.18 ± 0.01	min
$3^1 0^+ \rightarrow 5^1 0^-$	8538 ± 5	0.98 ± 0.06	max
$4^1 0^+ \rightarrow 2^1 0^-$	666000 ± 190000	0.008 ± 0.004	min
$4^1 0^+ \rightarrow 3^1 0^-$	18000 ± 12	0.0188 ± 0.0002	min
$4^1 0^+ \rightarrow 3^1 0^-$	52800 ± 110	6.6 ± 0.3	min
$4^1 0^+ \rightarrow 4^1 0^-$	13850 ± 200	0.032 ± 0.002	min
$4^1 0^+ \rightarrow 4^1 0^-$	41630 ± 220	1.75 ± 0.01	max
$4^1 0^+ \rightarrow 5^1 0^-$	11530 ± 100	0.025 ± 0.002	min
$4^1 0^+ \rightarrow 5^1 0^-$	22750 ± 30	1.28 ± 0.02	max
$4^1 0^+ \rightarrow 6^1 0^-$	9730 ± 12	0.0239 ± 0.0003	min
$5^1 0^+ \rightarrow 4^1 0^-$	25000 ± 2000	0.059 ± 0.001	min
$5^1 0^+ \rightarrow 5^1 0^-$	34390 ± 40	0.0085 ± 0.0015	max
$5^1 0^+ \rightarrow 5^1 0^-$	23000 ± 600	0.067 ± 0.005	min

Table 8: Same as Table 7 but for the triplet transitions $\mu^3 0^+ \rightarrow \nu^3 0^-$ for $\mu = 1, \dots, 4$, $\nu = 1, \dots, 6$

Component $\nu^{2S+1}M^{(-1)\Pi_z}$	wavelength/Å	position $B/a.u.$	max/min
$1^3 0^+ \rightarrow 1^3 0^-$	1869 ± 5	40 ± 2	min
$1^3 0^+ \rightarrow 2^3 0^-$	3184 ± 3	0.224 ± 0.005	min
$1^3 0^+ \rightarrow 2^3 0^-$	4289 ± 3.5	2.25 ± 0.02	max
$1^3 0^+ \rightarrow 3^3 0^-$	2503 ± 3	0.281 ± 0.005	min
$1^3 0^+ \rightarrow 3^3 0^-$	2837 ± 2	1.51 ± 0.01	max
$1^3 0^+ \rightarrow 4^3 0^-$	2292 ± 3	0.293 ± 0.005	min
$1^3 0^+ \rightarrow 4^3 0^-$	2522 ± 1	1.39 ± 0.01	max
$1^3 0^+ \rightarrow 5^3 0^-$	2197 ± 5	0.299 ± 0.005	min
$1^3 0^+ \rightarrow 5^3 0^-$	2394 ± 1	1.34 ± 0.02	max
$2^3 0^+ \rightarrow 2^3 0^-$	56500 ± 2100	0.05 ± 0.01	max
$2^3 0^+ \rightarrow 2^3 0^-$	39900 ± 300	0.17 ± 0.01	min
$2^3 0^+ \rightarrow 2^3 0^-$	12090 ± 25	26.6 ± 0.3	min
$2^3 0^+ \rightarrow 3^3 0^-$	9347 ± 3	0.24 ± 0.01	min
$2^3 0^+ \rightarrow 3^3 0^-$	16130 ± 45	3.65 ± 0.15	max
$2^3 0^+ \rightarrow 4^3 0^-$	6990 ± 10	0.26 ± 0.01	min
$2^3 0^+ \rightarrow 4^3 0^-$	9180 ± 5	2.23 ± 0.06	max
$2^3 0^+ \rightarrow 5^3 0^-$	6186 ± 10	0.27 ± 0.01	min
$2^3 0^+ \rightarrow 5^3 0^-$	7630 ± 3.5	1.87 ± 0.05	max
$3^3 0^+ \rightarrow 3^3 0^-$	18000 ± 2000	0.026 ± 0.003	min
$3^3 0^+ \rightarrow 3^3 0^-$	37428 ± 80	20.5 ± 0.5	min
$3^3 0^+ \rightarrow 4^3 0^-$	12400 ± 1000	0.039 ± 0.003	min
$3^3 0^+ \rightarrow 4^3 0^-$	22200 ± 100	0.14 ± 0.02	max
$3^3 0^+ \rightarrow 4^3 0^-$	21650 ± 50	0.25 ± 0.02	min
$3^3 0^+ \rightarrow 4^3 0^-$	40600 ± 40	4.5 ± 0.3	max
$3^3 0^+ \rightarrow 5^3 0^-$	10400 ± 300	0.030 ± 0.002	min
$3^3 0^+ \rightarrow 5^3 0^-$	15950 ± 100	0.135 ± 0.015	max
$3^3 0^+ \rightarrow 5^3 0^-$	15450 ± 50	0.275 ± 0.015	min
$3^3 0^+ \rightarrow 5^3 0^-$	21000 ± 55	2.6 ± 0.3	max
$3^3 0^+ \rightarrow 6^3 0^-$	9400 ± 100	0.032 ± 0.002	min
$4^3 0^+ \rightarrow 3^3 0^-$	477000 ± 15000	0.0225 ± 0.0015	max
$4^3 0^+ \rightarrow 3^3 0^-$	150000 ± 90000	0.08 ± 0.02	min
$4^3 0^+ \rightarrow 4^3 0^-$	96500 ± 1000	0.0062 ± 0.0002	max
$4^3 0^+ \rightarrow 4^3 0^-$	20150 ± 300	0.064 ± 0.001	min
$4^3 0^+ \rightarrow 4^3 0^-$	206000 ± 5000	0.17 ± 0.03	max
$4^3 0^+ \rightarrow 4^3 0^-$	181000 ± 12000	0.26 ± 0.04	min
$4^3 0^+ \rightarrow 5^3 0^-$	31400 ± 400	0.014 ± 0.001	max
$4^3 0^+ \rightarrow 5^3 0^-$	16800 ± 500	0.068 ± 0.005	min
$4^3 0^+ \rightarrow 5^3 0^-$	44700 ± 3000	0.18 ± 0.02	max
$4^3 0^+ \rightarrow 5^3 0^-$	38000 ± 6000	0.31 ± 0.03	min

References

- [1] H. Friedrich, Phys.Rev. **A 26**, 1827 (1982)
- [2] W. Rösner, G. Wunner, H. Herold and H. Ruder, J.Phys. **B 17**, 29 (1984)
- [3] D. Wintgen and H. Friedrich, J.Phys. **B 19**, 991 (1986)
- [4] M.V. Ivanov, J.Phys. **B 21**, 447 (1988)
- [5] Yu.P. Kravchenko, M.A. Liberman and B. Johansson, Phys.Rev. **A 54**, 287 (1996)
- [6] H. Ruder, G. Wunner, H. Herold und F. Geyer, Atoms in Strong Magnetic Fields, Springer Verlag A-A 1994.
- [7] P. Schmelcher and W. Schweizer, Atoms and Molecules in Strong External Fields, Plenum Press 1998
- [8] R.F. Green and J. Liebert, Pub. Astr. Soc. Pac 93, 105 (1980)
- [9] G.D. Schmidt et al. **ApJ** 350, 758 (1990)
- [10] S. Jordan, P. Schmelcher, W. Becken and W. Schweizer, Astronomy & Astrophysics Letters **336**, L33-L36 (1998)
- [11] G. Thurner, H. Herold, H. Ruder, G. Schlicht and G. Wunner, Phys. Letters, **89A**, no. 3, 133 (1982)
- [12] P. Pröschel, W. Rösner, G. Wunner, H. Ruder and H. Herold, J.Phys. **B 15**, 1959 (1982)
- [13] G. Thurner, H. Körbel, M. Braun, H. Herold, H. Ruder and G. Wunner, J.Phys. **B 26**, 4719 (1993)
- [14] M.V. Ivanov, Opt. Spectrosc. (USSR) **70** (2) (1991)
- [15] J. Virtamo, J.Phys. **B 9**, 751 (1976)
- [16] M.V. Ivanov, J.Phys. **B 27**, 4513 (1994)
- [17] M.D. Jones, G. Ortiz, D.M. Ceperley, Phys. Rev. **A 54**, 219 (1996)
- [18] R.O. Mueller, A.R.P. Rau and L. Spruch Phys. Rev. **A 11** 789 (1975)
- [19] M. Vincke and D. Baye, J. Phys **B 22** 2089 (1989)
- [20] D.M. Larsen, Phys.Rev. **B 20**, 20 (1979)
- [21] C.-H. Park and A.F. Starace, Phys.Rev. **A 29**, 442 (1984)
- [22] M.D. Jones, G. Ortiz, D.M. Ceperley, Phys.Rev. **E 55**, 6202 (1997)
- [23] M. Braun, W. Schweizer, H. Elster, Phys.Rev. **A 57**, 3739 (1998)
- [24] P. Schmelcher and L.S. Cederbaum, Phys.Rev. **A 37**, 672 (1988)
- [25] U. Kappes and P. Schmelcher, J.Chem.Phys. **100**, 2878 (1994); Phys.Rev. **A 51**, 4542 (1995); Phys.Rev. **A 53**, 3869 (1996)

- [26] T. Detmer, P. Schmelcher, F.K. Diakonos and L.S. Cederbaum, Phys.Rev. **A 56**, 1825 (1997)
- [27] T. Detmer, P. Schmelcher, L.S. Cederbaum, Phys.Rev. **A 57**, 1767 (1998)
- [28] A. Scrinzi, *private communications*
- [29] M. Braun, W. Schweizer and H. Herold, Phys.Rev.**A 48**, 1916 (1993)
- [30] Y. Accad and C.L. Pekeris, Phys.Rev. **A 24**, 516 (1971)
- [31] G.W.F. Drake and Z.-C. Yan, Phys.Rev. **A 46** 2378 (1992)
- [32] Z. Chen and S.P. Goldman, Phys. Rev. **A 45**, 1722 (1992)
- [33] V.B. Pavlov-Verevkin and B.I. Zhilinskii, Phys. Letters, **78A**, no. 3, 244 (1980)
- [34] B.R. Johnson, J.O. Hirschfelder and K.-H. Yang, Reviews of Modern Physics **55**, 109 (1983)
- [35] P. Schmelcher, L.S. Cederbaum and U. Kappes, Conceptual Trends in Quantum Chemistry, Kluwer Academic Publisher 1994, p.1-51
- [36] P. Schmelcher and L.S. Cederbaum, Phys.Rev. **A 43**, 287 (1991)
- [37] W.B. Westerveld, F.B. Kets, H.G.M. Heideman and J. van Eck, J.Phys. **B 12** 15 2575 (1979)
- [38] J. von Neumann und E.P. Wigner, Eigenwerte bei adiabatischen Prozessen, Physik. Zeitschrift. **XXX**, 467 (1929)
- [39] J.D. Baker, D.E. Freund, R.N. Hill and J.D. Morgan III, Phys. Rev.**A 41**, 1247 (1990)
- [40] J.D. Baker, R.N. Hill and J.D. Morgan III, in *Relativistic, Quantum Electrodynamical, and Weak Interaction Effects in Atoms*, edited by Walter Johnson, Peter Mohr, and Joseph Sucher, AIP Conf. Proc. No. 189 (American Institute of Physics, New York, 1989), pp. 123-145.
- [41] W. Becken and P. Schmelcher, *in preparation*
- [42] K. Singer, Proc. R. Soc. Lond. **A 402**, 412 (1960)
- [43] M. Abramowitz and I.A. Stegun, Handbook of mathematical functions, Dover Publications, 1972
- [44] Appell et Kampé de Fériet, Les fonctions hypergéométriques et hypersphériques, Gauthier-Villars et Cie, Editeurs, Paris 1926